Reunión Anual de la División de Partículas y Campos
RADPyC 2026

June 17, 2026

τ data-data based evaluation of the HVP

Alejandro Miranda
Cinvestav, México

Phys.Rev.D 102 (2020) 114017
Phys.Lett.B 850 (2024) 138492
Phys.Rev.D 111 (2025) 7, 073004
Phys.Rept. 1143 (2025) 1-158

The Anomalous Magnetic Moment of the Muon

WP20 - Phys. Rept. 887 (2020) 1-166

Contributions from known particles: The Standard Model

$$a_\mu(\text{SM}) = a_\mu(\text{QED}) + a_\mu(\text{Weak}) + a_\mu(\text{Hadronic})$$

QED 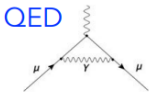 +…	$116\,584\,718.9\,(1) \times 10^{-11}$	0.001 ppm
Weak 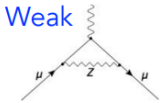 +…	$153.6\,(1.0) \times 10^{-11}$	0.01 ppm
Hadronic…		
…Vacuum Polarization (HVP) α^2 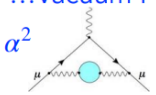 +…	$6845\,(40) \times 10^{-11}$ [0.6%]	0.37 ppm
…Light-by-Light (HLbL) α^3 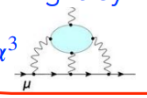 +…	$92\,(18) \times 10^{-11}$ [20%]	0.15 ppm

Numbers from Theory Initiative Whitepaper

Uncertainty dominated by hadronic contributions

C. Lehner. CERN EP seminar, 8 April 2021

a_μ=(g-2)/2 =Muon (magnetic) anomaly

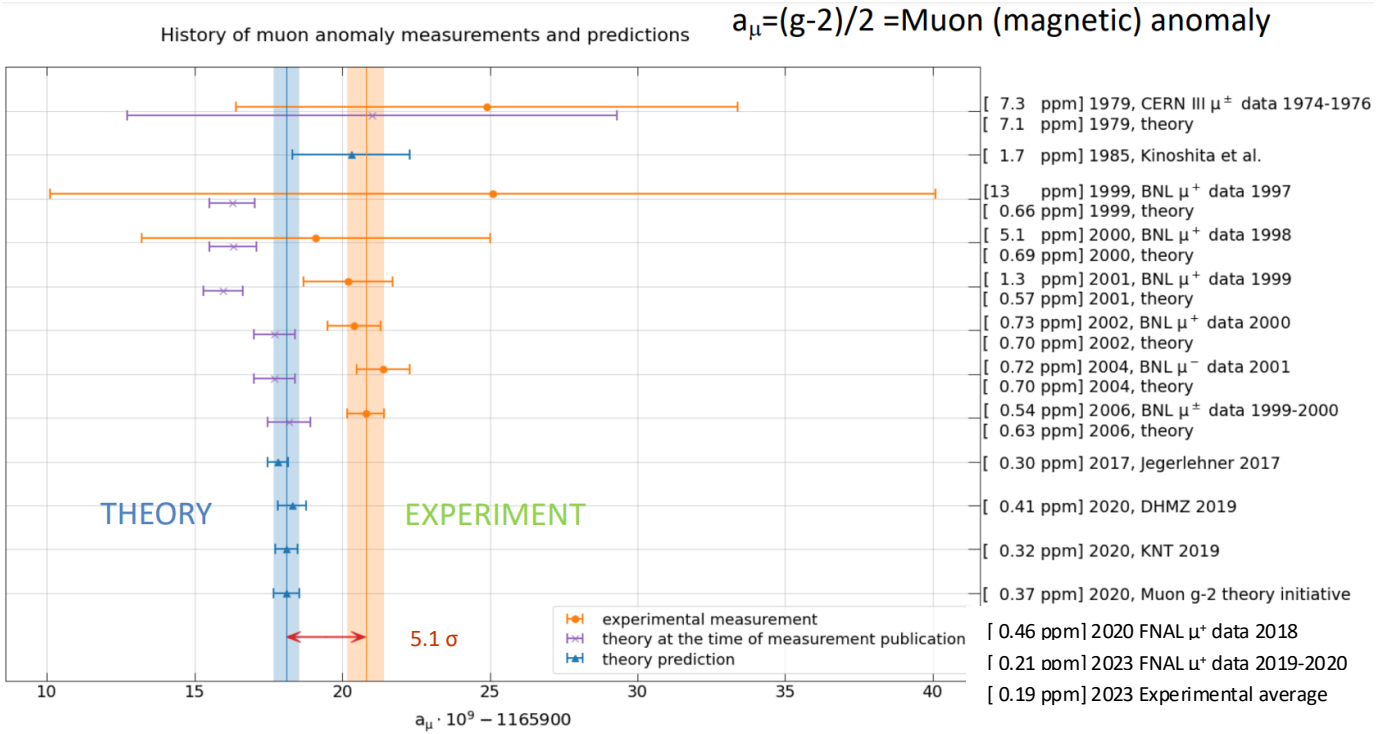

G. Venanzoni. CERN seminar, 8 April 2021

The Anomalous Magnetic Moment of the Muon

WP24 - Phys. Rept. 1143 (2025) 1-158

Contributions from known particles: The Standard Model

$$a_\mu(\text{SM}) = a_\mu(\text{QED}) + a_\mu(\text{Weak}) + a_\mu(\text{Hadronic})$$

QED +…	$116\,584\,718.8\,(2) \times 10^{-11}$	0.002 ppm
Weak +…	$154.4\,(4) \times 10^{-11}$	0.003 ppm
Hadronic…		
…Vacuum Polarization (HVP) α^2 +…	$7045\,(61) \times 10^{-11}$ [0.87%]	0.52 ppm
…Light-by-Light (HLbL) α^3 +…	$115.5\,(9.9) \times 10^{-11}$ [8.6%]	0.08 ppm

Numbers from Theory Initiative Whitepaper

Uncertainty dominated by hadronic contributions

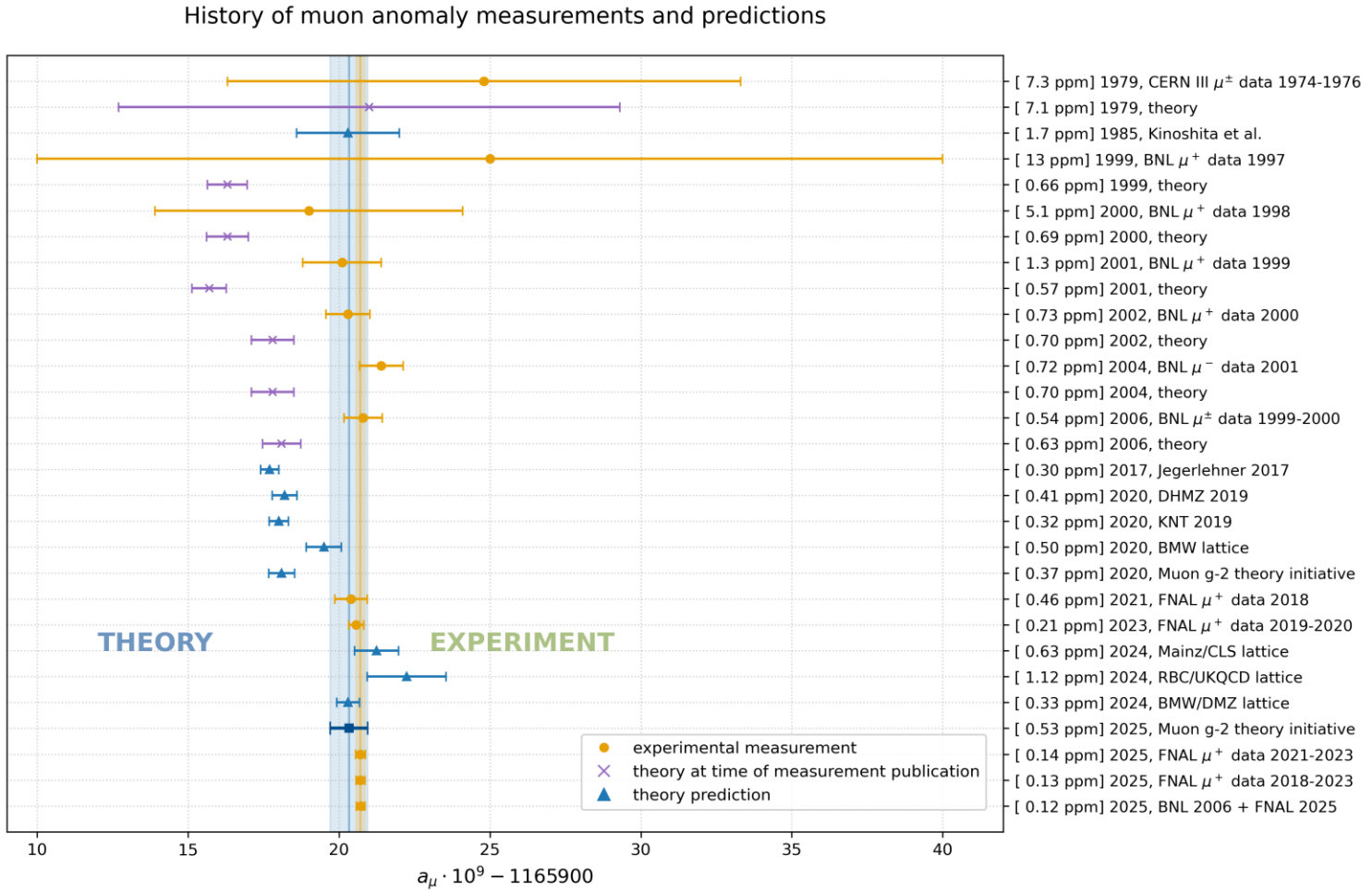

The Anomalous Magnetic Moment of the Muon

WP24 - Phys. Rept. 1143 (2025) 1-158

Contributions from known particles: The Standard Model

$$a_\mu(\text{SM}) = a_\mu(\text{QED}) + a_\mu(\text{Weak}) + a_\mu(\text{Hadronic})$$

QED 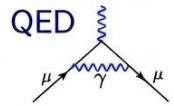 +…	$116\,584\,718.8\,(2) \times 10^{-11}$	0.002 ppm
Weak 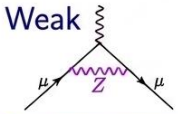 +…	$154.4\,(4) \times 10^{-11}$	0.003 ppm
Hadronic…		
…Vacuum Polarization (HVP) α^2 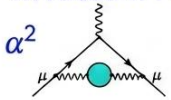 +…	$7045\,(61) \times 10^{-11}$ [0.87%]	0.52 ppm
…Light-by-Light (HLbL) α^3 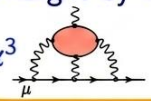 +…	$115.5\,(9.9) \times 10^{-11}$ [8.6%]	0.08 ppm

Numbers from Theory Initiative Whitepaper

Uncertainty dominated by hadronic contributions

History of muon anomaly measurements and predictions

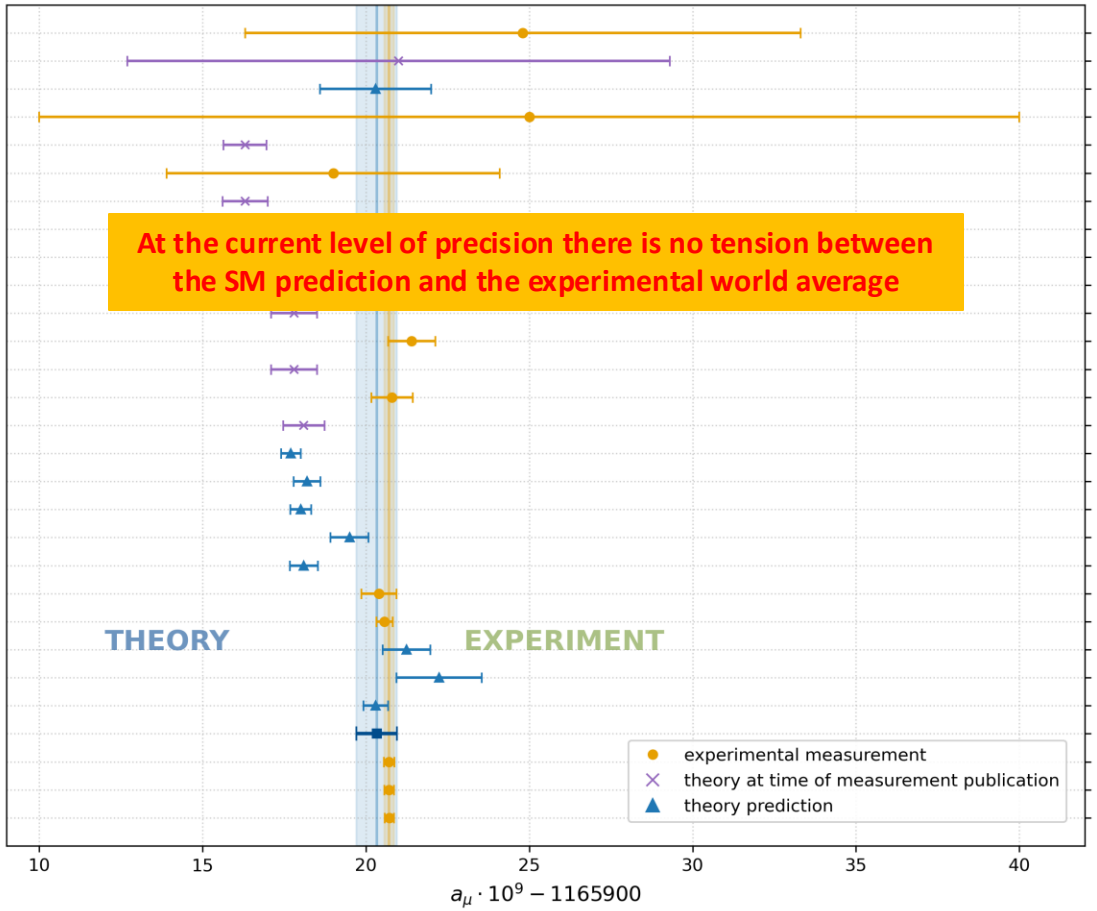

The E34 experiment at J-PARC/Japan aim to perform ultra-precision measurements of g-2 and EDM by using a different method.

Hadronic vacuum polarization

- At low energies **QCD** gets **strongly interacting** and a **perturbative calculation** is **not feasible**.
- Luckily, **analyticity** and **unitarity** allow us to express the **leading hadronic vacuum polarization** (**HVP**) contributions via a **dispersion relation** in terms of **experimental data**:

$$a_\mu^{\mathrm{HVP,LO}} = \frac{\alpha^2}{3\pi^2}\int_{m_\pi^2}^{\infty} ds \frac{K(s)}{s} R(s),$$

Gourdin, De Rafael. Nucl.Phys.B 10 (1969) 667-674

where **K(s)** is a **Kernel function** $\Longrightarrow$ $K(s) \sim 1/s,$

$$R(s) = \frac{\sigma^0(e^+e^- \to \mathrm{hadrons}(+\gamma))}{\sigma_{pt}}, \quad \sigma_{pt} = \frac{4\pi\alpha^2}{3s}$$

- An evaluation of the **HVP, LO** contribution can be obtained from the measurements of **$\sigma(e^+e^- \to$ hadrons)** or the **$\tau \to \nu_\tau$ + hadron** decays which can be related to the **isovector component** of the **$e^+e^- \to$ hadrons** cross section through **isospin-symmetry**.

Hadronic vacuum polarization

- At low energies **QCD** gets **strongly interacting** and a **perturbative calculation** is **not feasible**.
- Luckily, **analyticity** and **unitarity** allow us to express the **leading hadronic vacuum polarization** (**HVP**) contributions via a **dispersion relation** in terms of **experimental data**:

$$a_\mu^{\mathrm{HVP,LO}} = \frac{\alpha^2}{3\pi^2}\int_{m_\pi^2}^{\infty} ds \frac{K(s)}{s} R(s),$$

Gourdin, De Rafael. Nucl.Phys.B 10 (1969) 667-674

where ***K(s)*** is a **Kernel function** $\Longrightarrow$ $K(s) \sim 1/s,$

$$R(s) = \frac{\sigma^0(e^+e^- \to \mathrm{hadrons}(+\gamma))}{\sigma_{pt}}, \quad \sigma_{pt} = \frac{4\pi\alpha^2}{3s}$$

- An evaluation of the **HVP, LO** contribution can be obtained from the measurements of **$\sigma(e^+e^- \to \mathrm{hadrons})$** or the **$\tau \to \nu_\tau$ + hadron** decays which can be related to the **isovector component** of the **$e^+e^- \to \mathrm{hadrons}$** cross section through **isospin-symmetry**.
- Since both are subject to **theoretical uncertainties**, it is a good strategy to keep using both.

Hadronic vacuum polarization

- About **73%** of the contributions to the **HVP** and **58%** of the total uncertainty correspond to the **$\pi^+\pi^-(\gamma)$** final state at **low energies** ($4m_\pi^2 \leq s \leq 0.8\,\mathrm{GeV}^2$).
- For the **two-pion** final state,

$$\sigma_{\pi^+\pi^-}(s) = \frac{\pi\alpha^2\beta^3_{\pi^-\pi^+}(s)}{3s}\,|F_V(s)|^2\,,$$

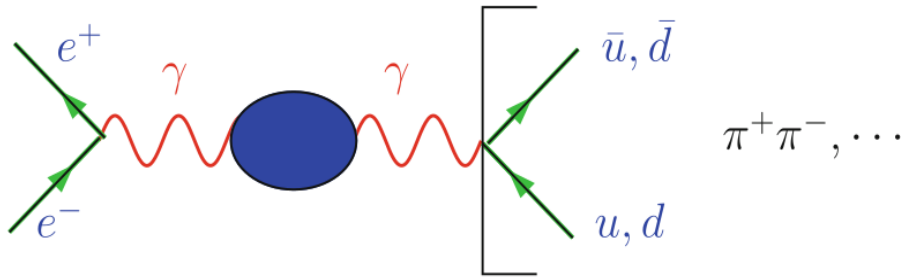

F. Jegerlehner. Springer Tracts Mod.Phys. 274 (2017)

Hadronic vacuum polarization

- About **73%** of the contributions to the **HVP** and **58%** of the total uncertainty correspond to the **$\pi^+\pi^-(\gamma)$** final state at **low energies** ($4m_\pi^2 \leq s \leq 0.8\,\mathrm{GeV}^2$).
- For the **two-pion** final state,

$$\sigma_{\pi^+\pi^-}(s) = \frac{\pi\alpha^2\beta^3_{\pi^-\pi^+}(s)}{3s}\,|F_V(s)|^2\,,$$

- Including **isospin-breaking corrections** at LO, we have

$$\sigma_{\pi^+\pi^-}(s) = \left[\frac{K_\sigma(s)}{K_\Gamma(s)}\frac{d\Gamma_{\pi\pi[\gamma]}}{ds}\right]\frac{R_{IB}(s)}{S_{EW}}$$

Kinematics — Measurement — Short-distance EW RadCor

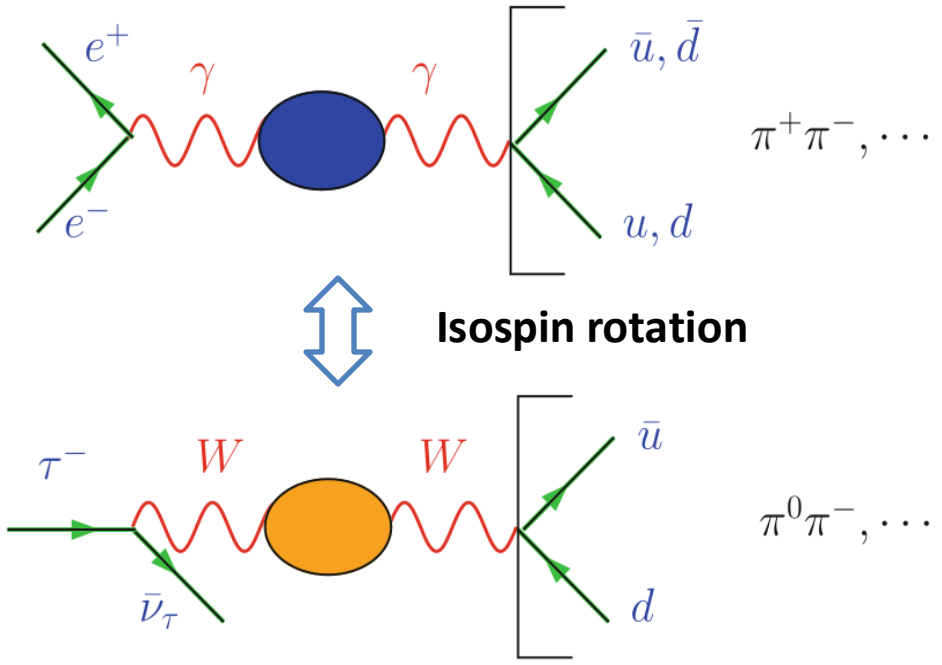

F. Jegerlehner. Springer Tracts Mod.Phys. 274 (2017)

Hadronic vacuum polarization

- About 73% of the contributions to the HVP and 58% of the total uncertainty correspond to the $\pi^+\pi^-(\gamma)$ final state at low energies $(4m_\pi^2 \leq s \leq 0.8\,\mathrm{GeV}^2)$.
- For the two-pion final state,

$$\sigma_{\pi^+\pi^-}(s) = \frac{\pi\alpha^2\beta^3_{\pi^-\pi^+}(s)}{3s}\,|F_V(s)|^2\,,$$

- Including isospin-breaking corrections at LO, we have

$$\sigma_{\pi^+\pi^-}(s) = \left[\frac{K_\sigma(s)}{K_\Gamma(s)}\frac{d\Gamma_{\pi\pi[\gamma]}}{ds}\right]\frac{R_{IB}(s)}{S_{EW}},$$

where $R_{IB}(s) = \frac{FSR(s)}{G_{EM}(s)}\frac{\beta^3_{\pi^+\pi^-}}{\beta^3_{\pi^0\pi^-}}\left|\frac{F_V(s)}{f_+(s)}\right|^2,$

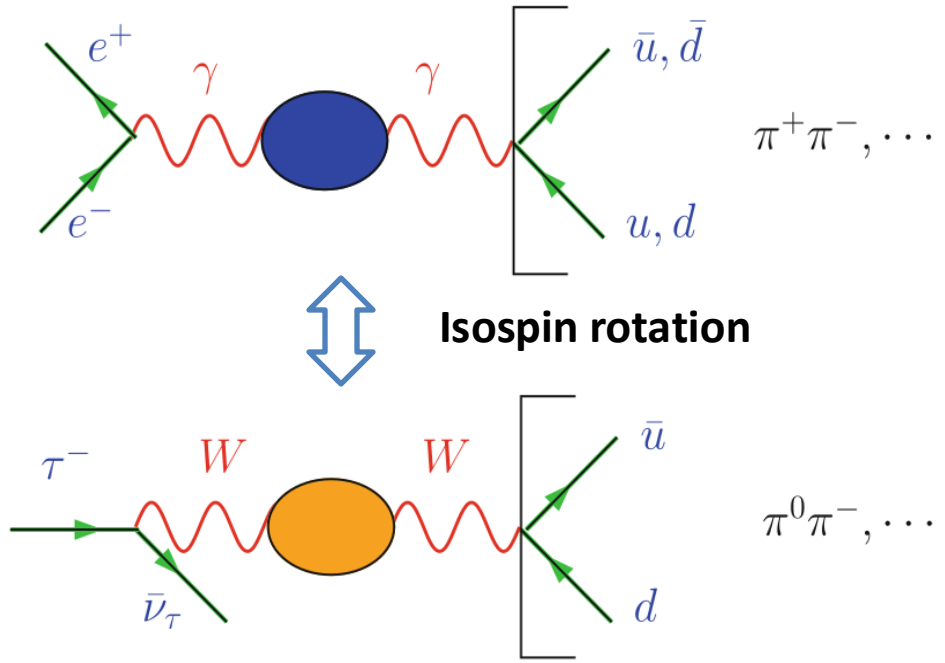

F. Jegerlehner. Springer Tracts Mod.Phys. 274 (2017)

- The ratio of neutral to charged current di-pion form factor and the long-distance em RadCor are challenging.
- $G_{EM}(s)$ receives contributions from real and virtual photons.

Cirigliano et al. Phy. Lett. B513 (2001). JHEP 08 (2002) 002

Hadronic vacuum polarization

- There is a **discrepancy** between the values of $a_\mu^{HVP,LO}[\pi\pi]$ obtained through e^+e^- and τ decays. According to Cirigliano et al. this could be a **NP effect**,

$$\frac{a_\mu^\tau - a_\mu^{ee}}{2\, a_\mu^{ee}} = \epsilon_L^{d\tau} - \epsilon_L^{de} + \epsilon_R^{d\tau} - \epsilon_R^{de} + c_T\, \hat{\epsilon}_T^{d\tau}$$

Phy. Rev. Lett. 122 (2019)
JHEP 04 (2022) 152

- There is a **solution** given by **Jegerlehner** and **Szafron** that induces an **additional correction** due to the $\rho - \gamma$ mixing where ρ^0 is regarded as a gauge boson.

Eur. Phys. J. C 71 (2011) 1632

- **NP effects** in $\tau^- \to \pi^- \pi^0 \nu_\tau$ decays were studied using an **EFT** framework for some observables.

JHEP 11 (2018) 038

- A **global fit** using **hadronic tau decays** to set bounds on **NP** effective couplings at the **low-energy** limit of **SMEFT** was performed by Gonzàlez-Solís et al.

Phys. Lett. B 804 (2020) 135371

Hadronic vacuum polarization

- There is a **discrepancy** between the values of $a_\mu^{HVP,LO}[\pi\pi]$ obtained through e^+e^- and τ decays. According to Cirigliano et al. this could be a **NP effect**,

$$\frac{a_\mu^\tau - a_\mu^{ee}}{2\, a_\mu^{ee}} = \epsilon_L^{d\tau} - \epsilon_L^{de} + \epsilon_R^{d\tau} - \epsilon_R^{de} + c_T\, \hat{\epsilon}_T^{d\tau}$$

Phy. Rev. Lett. 122 (2019)
JHEP 04 (2022) 152

- There is a **solution** given by **Jegerlehner** and **Szafron** that induces an **additional correction** due to the $\rho - \gamma$ mixing where ρ^0 is regarded as a gauge boson.

Eur. Phys. J. C 71 (2011) 1632

- **NP effects** in $\tau^- \to \pi^- \pi^0 \nu_\tau$ decays were studied using an **EFT** framework for some observables.

JHEP 11 (2018) 038

- A **global fit** using **hadronic tau decays** to set bounds on **NP** effective couplings at the **low-energy** limit of **SMEFT** was performed by Gonzàlez-Solís et al.

Phys. Lett. B 804 (2020) 135371

- Three **lattice calculations** (**BMW-20**, **Mainz/CLS-24**, and **RBC/UKQCD-24**) achieve uncertainties comparable to the e^+e^- result and **reduce the tension** with the **experimental measurement**.

Nature 593 (2021) 7857, 51-55

Hadronic vacuum polarization

- There is a **discrepancy** between the values of $a_\mu^{HVP,LO}[\pi\pi]$ obtained through e^+e^- and τ decays. According to Cirigliano et al. this could be a **NP effect**,

$$\frac{a_\mu^\tau - a_\mu^{ee}}{2\, a_\mu^{ee}} = \epsilon_L^{d\tau} - \epsilon_L^{de} + \epsilon_R^{d\tau} - \epsilon_R^{de} + c_T\, \hat{\epsilon}_T^{d\tau}$$

Phy. Rev. Lett. 122 (2019)
JHEP 04 (2022) 152

- There is a **solution** given by **Jegerlehner** and **Szafron** that induces an **additional correction** due to the $\rho - \gamma$ mixing where ρ^0 is regarded as a gauge boson.

Eur. Phys. J. C 71 (2011) 1632

- **NP effects** in $\tau^- \to \pi^- \pi^0 \nu_\tau$ decays were studied using an **EFT** framework for some observables.

JHEP 11 (2018) 038

- A **global fit** using **hadronic tau decays** to set bounds on **NP** effective couplings at the **low-energy** limit of **SMEFT** was performed by Gonzàlez-Solís et al.

Phys. Lett. B 804 (2020) 135371

- Three **lattice calculations** (**BMW-20**, **Mainz/CLS-24**, and **RBC/UKQCD-24**) achieve uncertainties comparable to the e^+e^- result and **reduce the tension** with the **experimental measurement**.

Nature 593 (2021) 7857, 51-55

- The **recent measurement** of the e^+e^- cross section by **CMD-3** is in conflict with all previous determinations.

Phys.Rev.D 109 (2024) 11, 112002

Long-distance radiative corrections

- G_{EM} was originally studied by **Cirigliano** et al in the frame of **RChT** at **O(p^4)**. JHEP 08 (2002) 002
- A recalculation was performed by **Flores-Baez** et al using a **VMD** model. Phys.Rev.D 74 (2006) 071301
- The two model predictions **disagree** due to the presence of diagrams involving the **ρωπ** vertex.
- We extend the **RChT** estimation including contributions up to **O(p^6)**. Phys. Rev. D 102 (2020) 114017

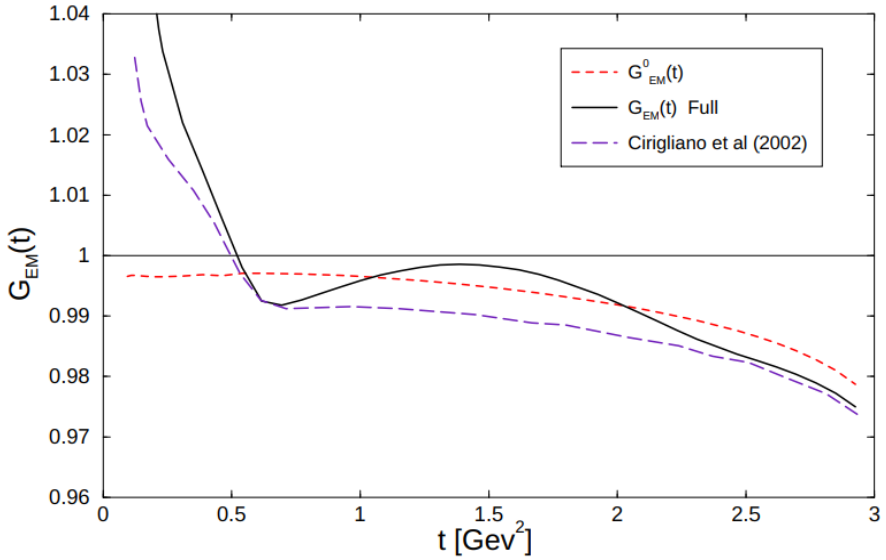

Nucl. Phys. B Proc.Suppl. 169 (2007) 250-254

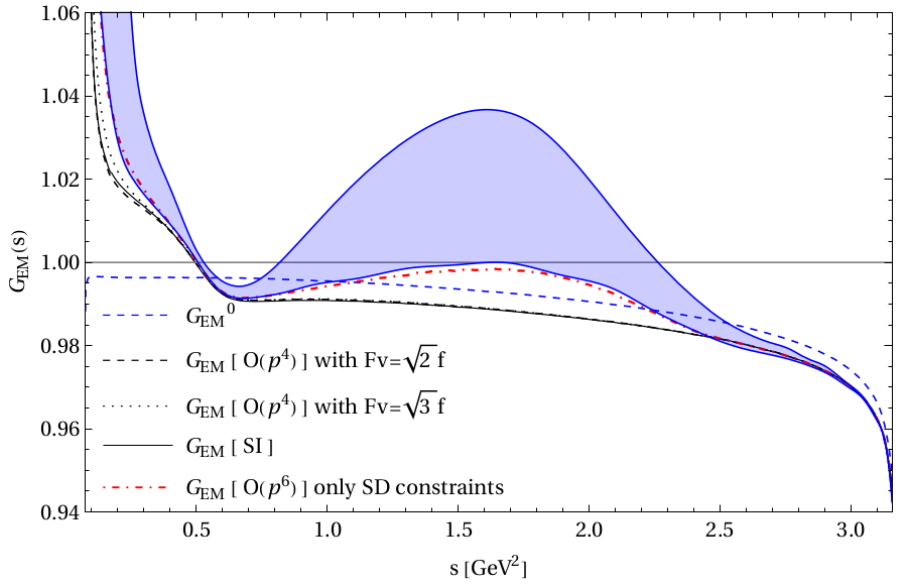

Data-driven calculations of HVP

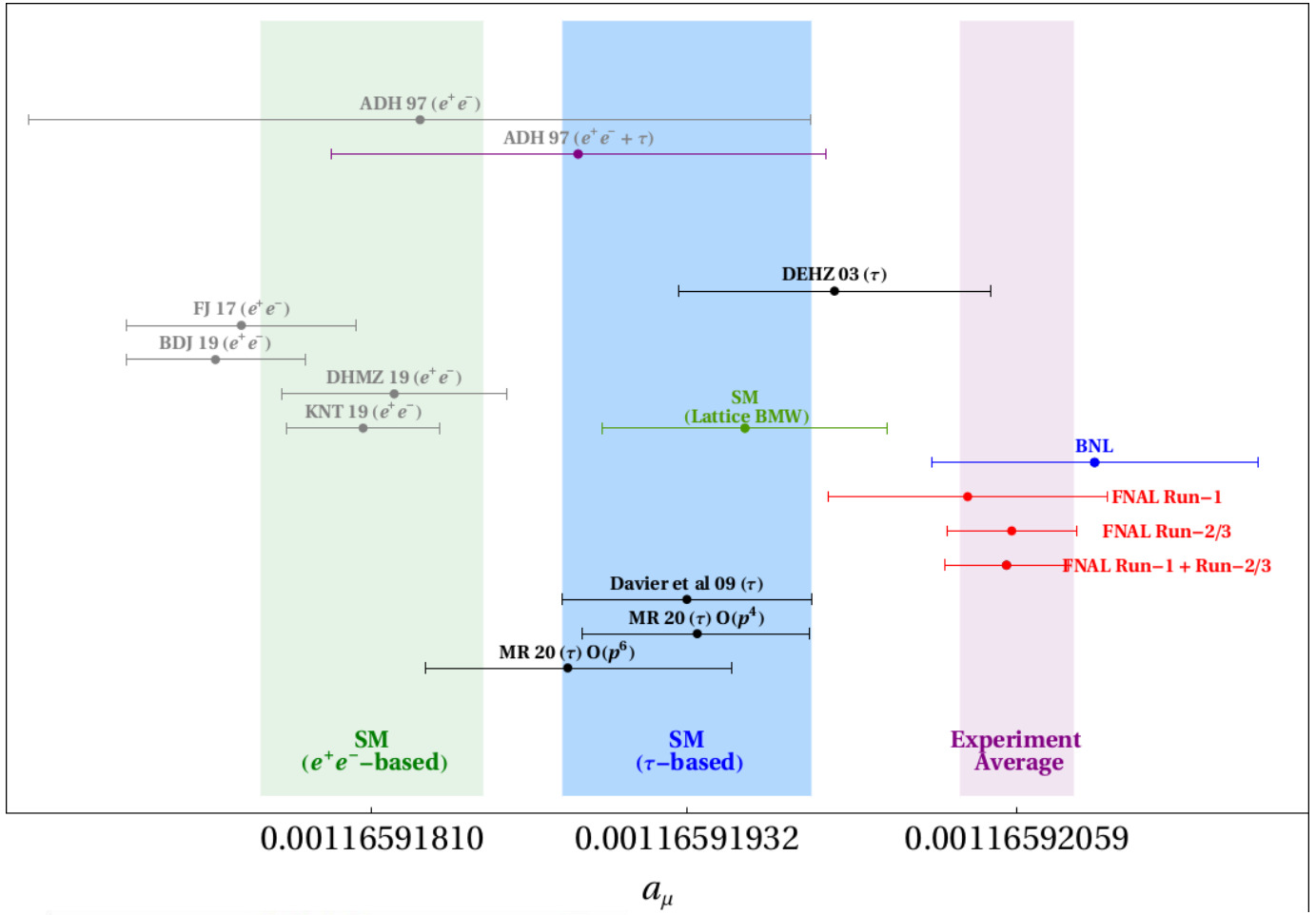

	$\Delta a_\mu^{\rm HVP,LO}[\pi\pi,\tau](\times 10^{10})$
Total	$-15.0(5.1)$

WP24 - Phys. Rept. 1143 (2025) 1-158

$$\sigma_{\pi^+\pi^-}(s) = \left[\frac{K_\sigma(s)}{K_\Gamma(s)}\frac{d\Gamma_{\pi\pi[\gamma]}}{ds}\right]\frac{R_{IB}(s)}{S_{EW}},$$

$$R_{IB}(s) = \frac{FSR(s)}{G_{EM}(s)}\frac{\beta^3_{\pi^+\pi^-}}{\beta^3_{\pi^0\pi^-}}\left|\frac{F_V(s)}{f_+(s)}\right|^2,$$

$\Delta a_\mu^{\rm HVP,LO}[\pi\pi,\tau](\times 10^{10})$		
Source	$\mathcal{O}(p^4)$	$\mathcal{O}(p^6)$
$S_{\rm EW}$	$-11.96(15)$	
PS	$-7.47(0)$	
FSR	$+4.56(46)$	
$G_{\rm EM}$	$-1.71(^{0.61}_{1.48})$	$-7.61(^{6.50}_{4.56})$
FF	$+7.13(1.48)(^{1.59}_{1.54})(^{85}_{80})$	
Total	$-9.45(^{2.51}_{2.83})$	$-15.35(^{6.98}_{5.17})$

S_{EW}: Sirlin '78; Marciano-Sirlin '93; Erler '04; Cirigliano et al '23
FF (Mixing,...) : Maltman '05; Maltman-Yorke '06, '11; Davier et al '09; López-Castro et al '24; Davier et al '25
EM: Cirigliano et al '01, '02; Flores-Tlalpa et al '06; Miranda and Roig '20; Esparza-Arellano et al '23; Cirigliano et al '26; Colangelo et al '26

Data-driven calculations of HVP

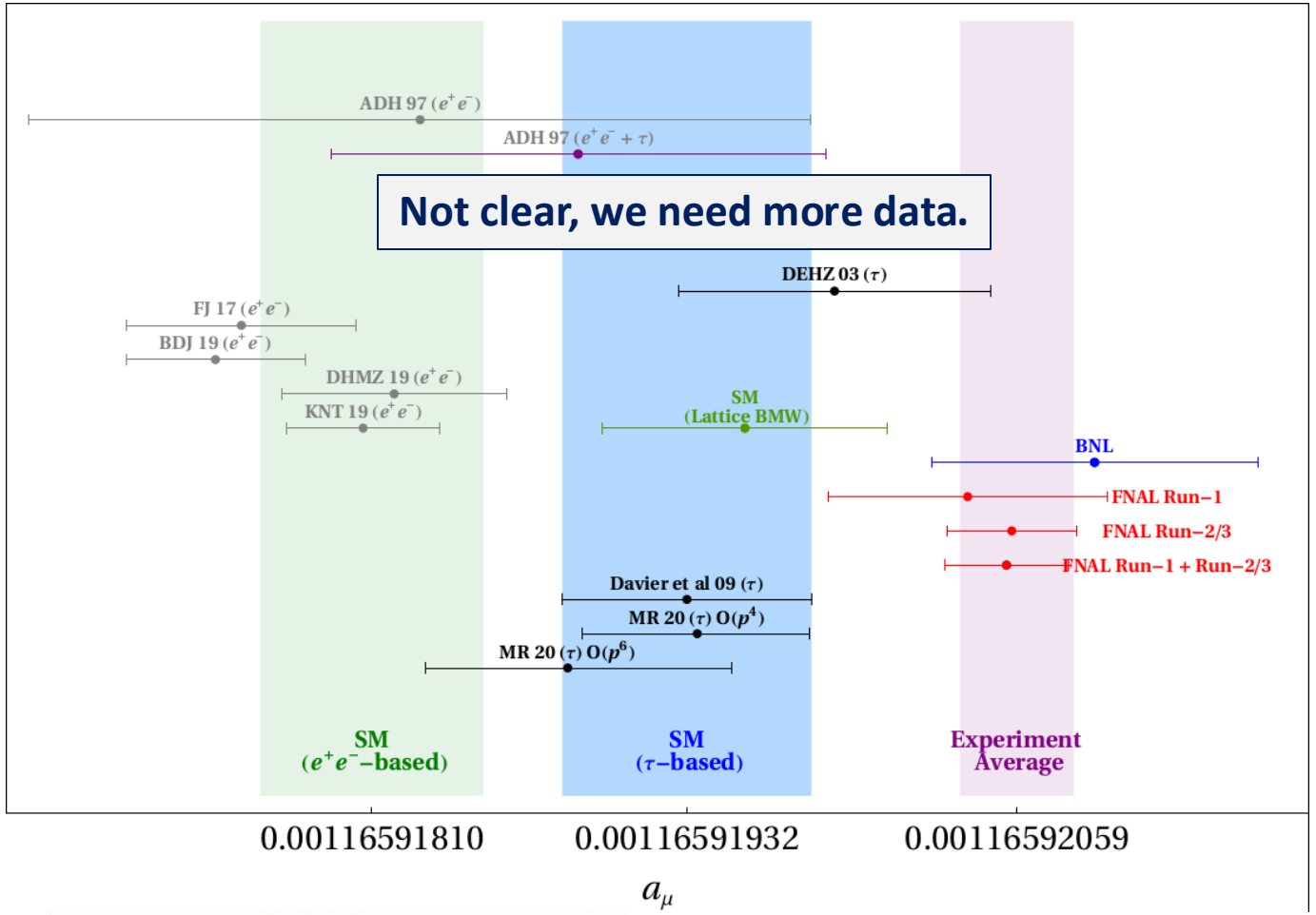

	$\Delta a_\mu^{\rm HVP,LO}[\pi\pi,\tau](\times 10^{10})$
Total	$-15.0(5.1)$

WP24 - Phys. Rept. 1143 (2025) 1-158

$$\sigma_{\pi^+\pi^-}(s) = \left[\frac{K_\sigma(s)}{K_\Gamma(s)}\frac{d\Gamma_{\pi\pi[\gamma]}}{ds}\right]\frac{R_{IB}(s)}{S_{EW}},$$

$$R_{IB}(s) = \frac{FSR(s)}{G_{EM}(s)}\frac{\beta^3_{\pi^+\pi^-}}{\beta^3_{\pi^0\pi^-}}\left|\frac{F_V(s)}{f_+(s)}\right|^2,$$

$\Delta a_\mu^{\rm HVP,LO}[\pi\pi,\tau](\times 10^{10})$		
Source	$\mathcal{O}(p^4)$	$\mathcal{O}(p^6)$
$S_{\rm EW}$	$-11.96(15)$	
PS	$-7.47(0)$	
FSR	$+4.56(46)$	
$G_{\rm EM}$	$-1.71(^{0.61}_{1.48})$	$-7.61(^{6.50}_{4.56})$
FF	$+7.13(1.48)(^{1.59}_{1.54})(^{85}_{80})$	
Total	$-9.45(^{2.51}_{2.83})$	$-15.35(^{6.98}_{5.17})$

S_{EW}: Sirlin '78; Marciano-Sirlin '93; Erler '04; Cirigliano et al '23
FF (Mixing,…) : Maltman '05; Maltman-Yorke '06, '11; Davier et al '09; López-Castro et al '24; Davier et al '25
EM: Cirigliano et al '01, '02; Flores-Tlalpa et al '06; Miranda and Roig '20; Esparza-Arellano et al '23; Cirigliano et al '26; Colangelo et al '26

HVP, LO from data

- Comparison of results for the **HVP, LO**, evaluated between **0.6 GeV** and **0.88 GeV** .

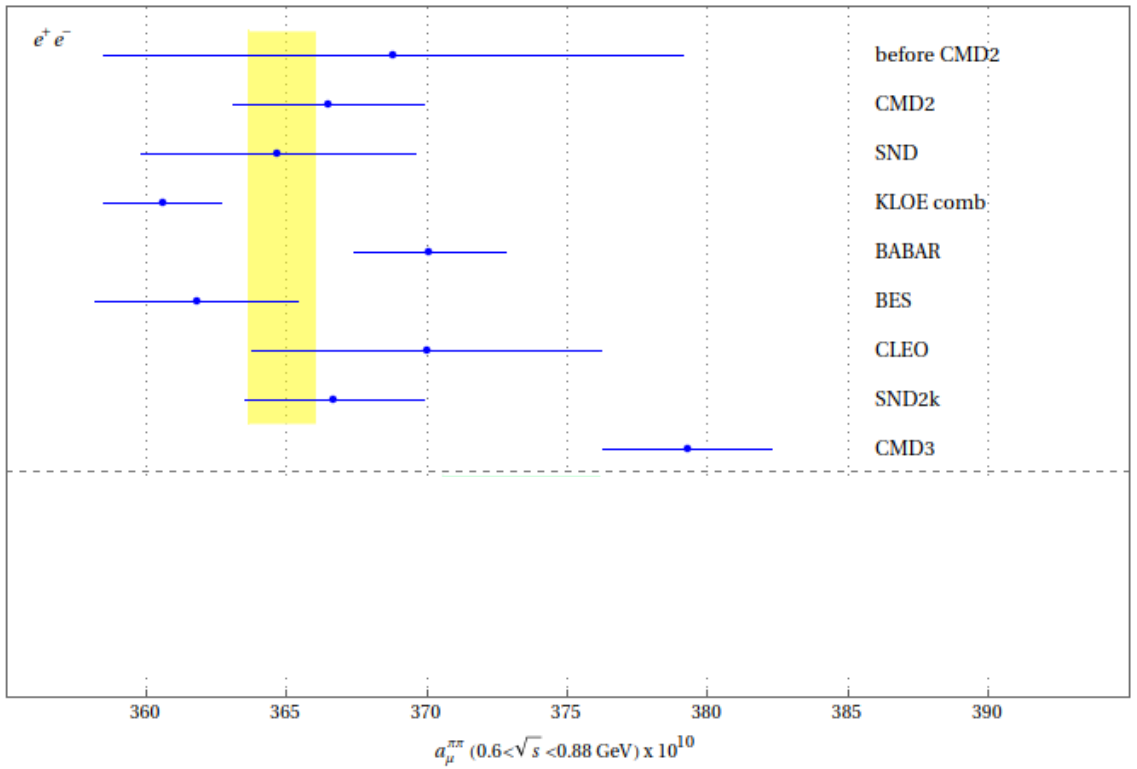

Experiment	$a_\mu^{\pi^+\pi^-,\mathrm{LO}} \cdot 10^{10}$
before CMD2	368.8 ± 10.3
CMD2	366.5 ± 3.4
SND	364.7 ± 4.9
KLOE	360.6 ± 2.1
BABAR	370.1 ± 2.7
BES	361.8 ± 3.6
CLEO	370.0 ± 6.2
SND2k	366.7 ± 3.2
CMD3	379.3 ± 3.0

CMD-3. Phys.Rev.D 109 (2024) 11, 112002

HVP, LO from data

- Comparison of results for the **HVP, LO**, evaluated between **0.6 GeV** and **0.88 GeV** .

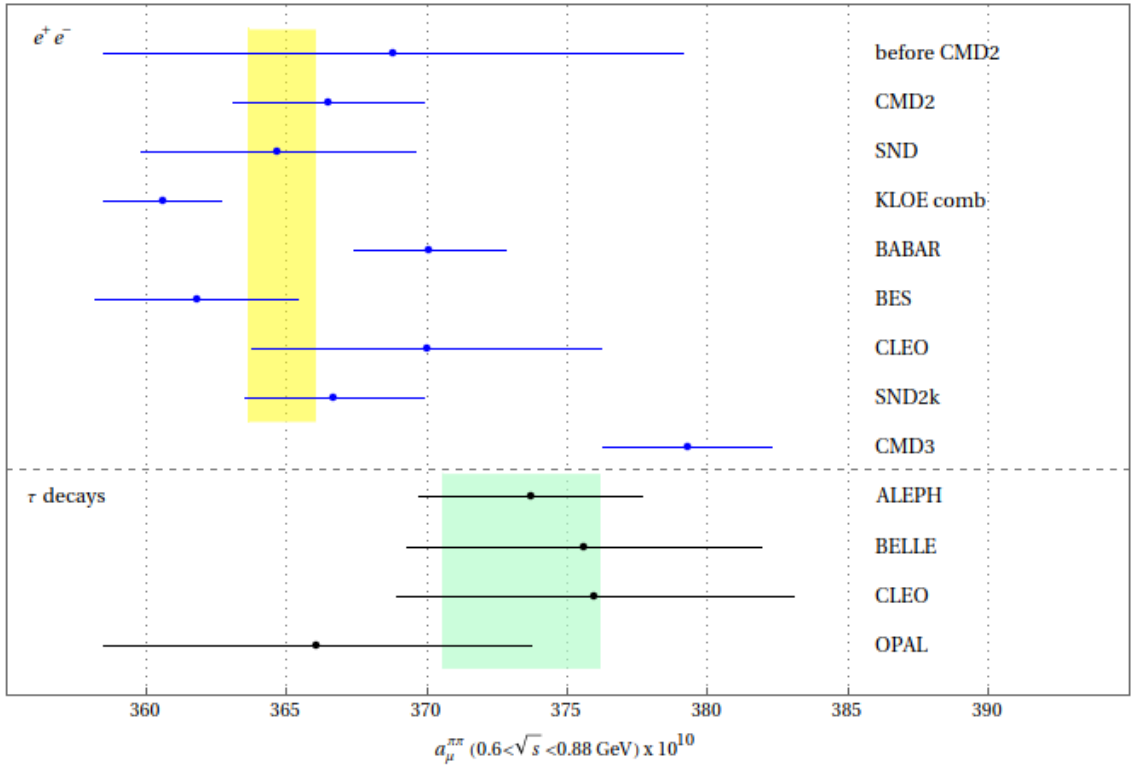

Experiment	$a_\mu^{\pi^+\pi^-,\mathrm{LO}} \cdot 10^{10}$
before CMD2	368.8 ± 10.3
CMD2	366.5 ± 3.4
SND	364.7 ± 4.9
KLOE	360.6 ± 2.1
BABAR	370.1 ± 2.7
BES	361.8 ± 3.6
CLEO	370.0 ± 6.2
SND2k	366.7 ± 3.2
CMD3	379.3 ± 3.0
ALEPH	373.7 ± 4.0
Belle	375.6 ± 6.3
CLEO	376.0 ± 7.1
OPAL	366.1 ± 7.6

e^+e^- data

τ data

CMD-3. Phys.Rev.D 109 (2024) 11, 112002

- Large tensions among experiments: **KLOE**, **BaBar** and **CMD3**.

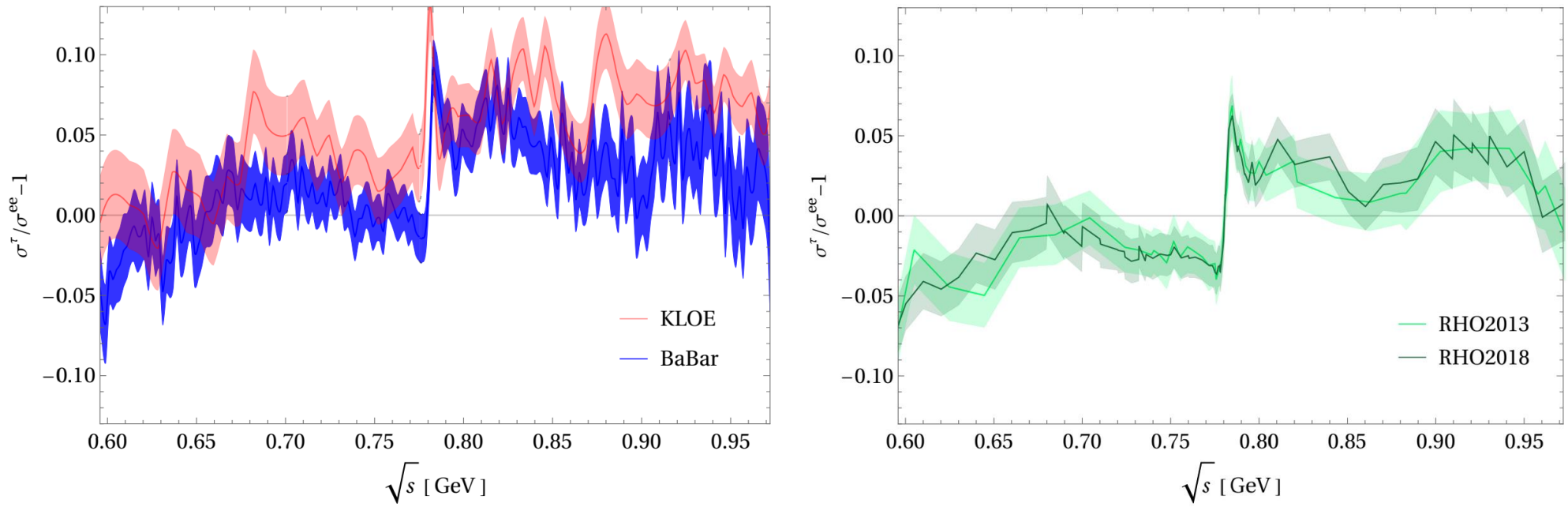

Comparison between the different data sets: KLOE and BaBar (left-hand) and CMD-3 (right-hand).

P. Masjuan. Phys.Lett.B 850 (2024) 138492

Euclidean windows

- **Euclidean window quantities** allow for the separation of the most challenging **short** and **long** time-distance contributions: **internal lattice cross-check**.

$$a_\mu = 4\alpha^2 \sum_t w_t \Big[\Theta_{\rm SD}(t) + \Theta_{\rm W}(t) + \Theta_{\rm LD}(t)\Big] G(t)$$

RBC/UKQCD 2018

- A **dispersive** result for the total **intermediate** window contribution,

$$a_\mu^{\rm W} = 229.4(1.4) \times 10^{-10}$$

which is in **4.3σ** tension with recent lattice results.

Phys.Lett.B 833 (2022) 137313

- The discrepancy between **data-driven** and **LQCD** is almost entirely due to the **light-quark connected** contribution, which is dominated by the **2π** channel **~81%**.

Phys.Rev.Lett. 131 (2023) 25, 251803

Before CMD-3

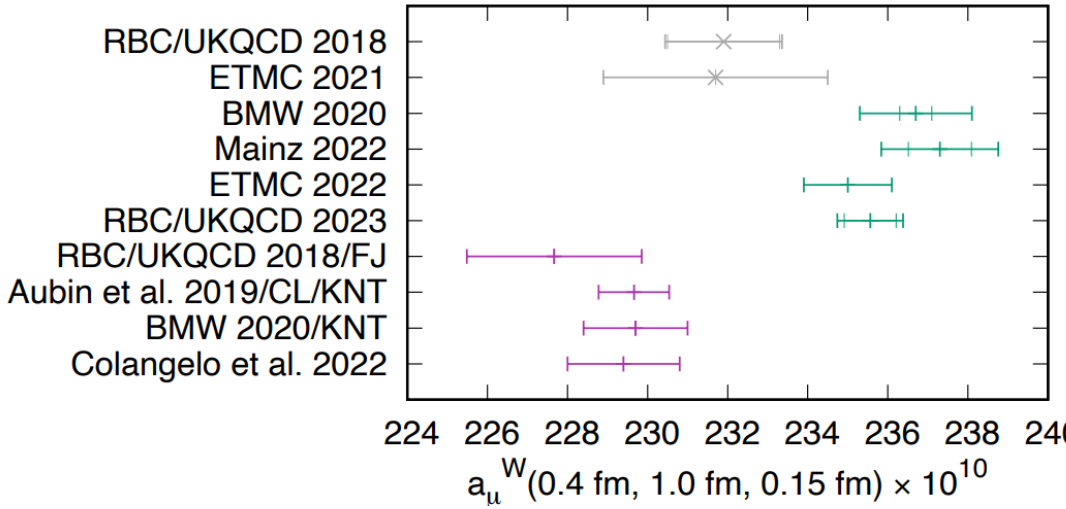

RBC/UKQCD 2023

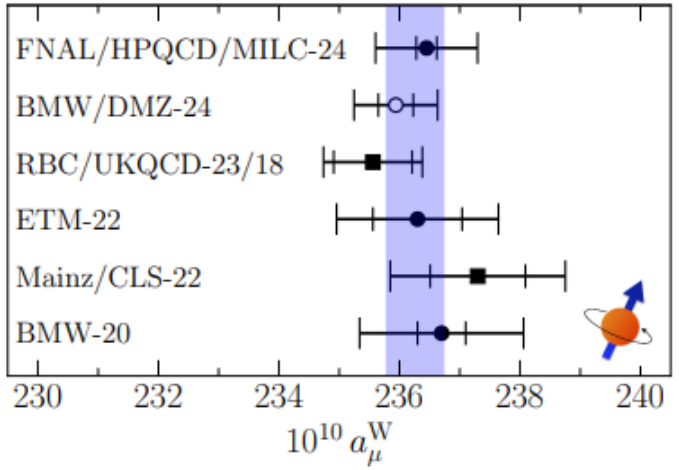

WP24 - Phys. Rept. 1143 (2025) 1-158

Windows quantities for 2π below 1.0 GeV

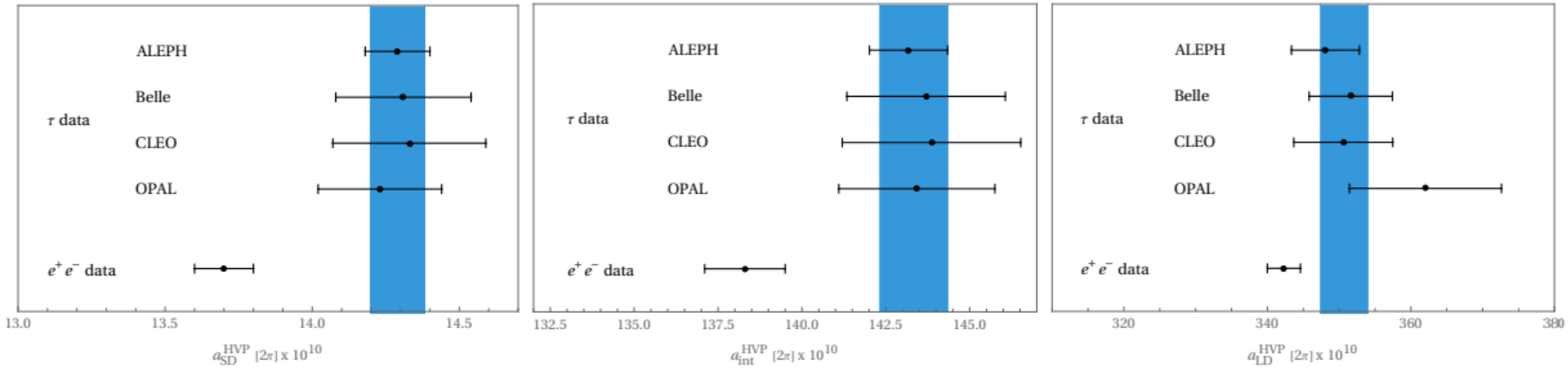

+ 4.3 σ
+ 3.2 σ
+ 2.1 σ

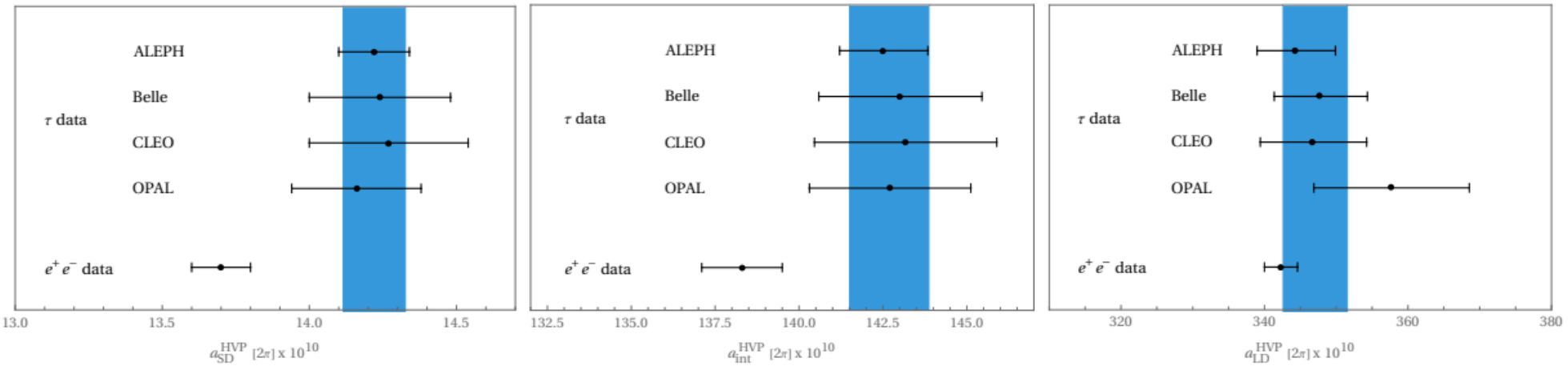

+ 3.6 σ
+ 2.6 σ
+ 0.9 σ

G. Colangelo. Phys.Lett.B 833 (2022) 137313

P. Masjuan. Phys.Lett.B 850 (2024) 138492

Hadronic vacuum polarization

- When **all other contributions** are added, we get the overall result for each **window quantity**.
- The contributions of the **intermediate window** using **tau data** are slightly closer to the **lattice** results (**~1.5σ**).

$a_\mu^{\mathrm{HVP,LO}}$				
	SD	int	LD	Total
τ-data $\mathcal{O}(p^4) \leq 1$ GeV	69.0(5)	$234.0(^{1.2}_{1.3})$	$402.5(^{3.3}_{3.4})$	$705.5(^{5.0}_{5.2})$
τ-data $\mathcal{O}(p^6) \leq 1$ GeV	68.9(5)	233.3(1.4)	$398.5(^{4.9}_{4.2})$	$700.7(^{6.8}_{6.1})$
τ-data $\mathcal{O}(p^4)$	69.0(7)	234.2(2.0)	$402.6(^{3.8}_{3.9})$	$705.8(^{6.5}_{6.6})$
τ-data $\mathcal{O}(p^6)$	68.9(7)	233.4(2.1)	$398.5(^{5.3}_{4.6})$	$700.8(^{8.1}_{7.4})$
RBC/UKQCD 2018 [12]	–	231.9(1.5)	–	715.4(18.7)
ETMC 2021 [148]	–	231.7(2.8)	–	–
BMW 2020 [66]	–	236.7(1.4)	–	707.5(5.5)
Mainz/CLS 2022 [67]	–	237.30(1.46)	–	–
ETMC 2022 [68]	69.33(29)	235.0(1.1)	–	–
RBC/UKQCD 2023 [62]	–	235.56(82)	–	–
WP [38]	–	–	–	693.1(4.0)
BMW 2020/KNT [4, 66]	–	229.7(1.3)	–	–
Colangelo et al. 2022 [69]	68.4(5)	229.4(1.4)	395.1(2.4)	693.0(3.9)
Davier et al. 2023 [e^+e^-] [147]	–	229.2(1.4)	–	694.0(4.0)
Davier et al. 2023 [τ] [125]	–	232.4(1.3)	–	–

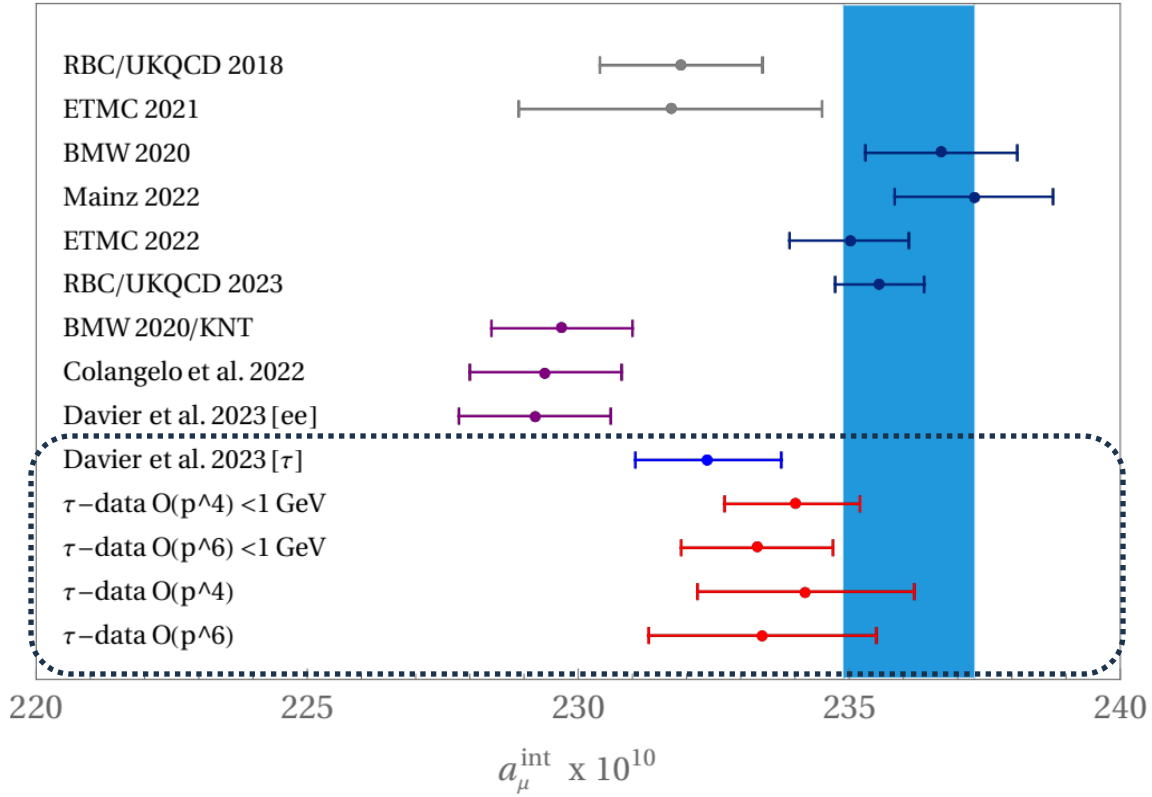

Isospin-breaking corrections

- We can **estimate** the effect of each **IB correction** through

$$\Delta a_\mu^{\mathrm{HVP,\ LO}}[\pi\pi,\tau] = \frac{1}{4\pi^3}\int_{4m_\pi^2}^{m_\tau^2} ds\, K(s)\left[\frac{K_\sigma(s)}{K_\Gamma(s)}\frac{d\Gamma_{\pi\pi[\gamma]}}{ds}\right]\left(\frac{R_{\mathrm{IB}}(s)}{S_{\mathrm{EW}}}-1\right),$$

$$R_{IB}(s) = \frac{FSR(s)}{G_{EM}(s)}\frac{\beta^3_{\pi^+\pi^-}}{\beta^3_{\pi^0\pi^-}}\left|\frac{F_V(s)}{f_+(s)}\right|^2,$$

Phys.Rev.D 111 (2025) 7, 073004

- $\Delta\Gamma_\rho = \Gamma_{\rho^0} - \Gamma_{\rho^\pm} = (1.8 \pm 0.2)$ MeV
- $\Delta\Gamma_\rho = -1.07$ MeV due to Δm_π
- $\Delta M_\rho = m_{\rho^\pm} - m_{\rho^0} = (1.0 \pm 0.9)$ MeV,

Eur. Phys. J. C 66, 127 (2010)

Fit results for the dispersive model

	BABAR12 + Belle	KLOE12 + Belle	KLOEc + Belle	CMD3 + Belle	Global fit 1	Global fit 2
Data points	322 + 62	60 + 62	85 + 62	209 + 62	322 + 60 + 209 + 62	322 + 85 + 209 + 62
χ^2	493.4	356.4	442.9	584.5	2192.2	2683.0
χ^2/d.o.f.	1.3	2.9	3.0	2.2	3.4	4.0
m_ρ	774.9 ± 0.1 MeV	774.9 ± 0.1 MeV	774.7 ± 0.1 MeV	774.9 ± 0.2 MeV	774.3 ± 0.1 MeV	774.1 ± 0.1 MeV
$\lvert\delta_{\rho\omega}\rvert$	$(2.0 \pm 0.0) \times 10^{-3}$	$(2.0 \pm 0.0) \times 10^{-3}$	$(2.0 \pm 0.0) \times 10^{-3}$	$(2.1 \pm 0.0) \times 10^{-3}$	$(2.1 \pm 0.0) \times 10^{-3}$	$(2.1 \pm 0.0) \times 10^{-3}$
$\arg[\delta_{\rho\omega}]$	$(17.2 \pm 0.9)°$	$(16.1 \pm 1.3)°$	$(25.0 \pm 2.3)°$	$(14.3 \pm 1.2)°$	$(13.3 \pm 0.4)°$	$(10.2 \pm 0.4)°$
$\lvert\delta_{\rho\phi}\rvert$	$0^\dagger$	$0^\dagger$	$0^\dagger$	$(2.0 \pm 0.1) \times 10^{-4}$	$(1.3 \pm 0.1) \times 10^{-4}$	$(1.7 \pm 0.2) \times 10^{-4}$
$\arg[\delta_{\rho\phi}]$	...	...	...	$(56.5 \pm 2.9)°$	$(22.9 \pm 5.3)°$	$(40.4 \pm 6.3)°$
C_2	-0.63 ± 0.00	-0.26 ± 0.00	-0.42 ± 0.01	-0.43 ± 0.00	$(-0.27 \pm 0.00) \times 10^{-1}$	-0.39 ± 0.02
C_3	0.37 ± 0.00	0.17 ± 0.00	0.29 ± 0.01	0.29 ± 0.01	$(0.28 \pm 0.00) \times 10^{-1}$	0.26 ± 0.01
C_4	-0.10 ± 0.00	-0.05 ± 0.00	-0.09 ± 0.00	-0.09 ± 0.01	$(-0.15 \pm 0.00) \times 10^{-1}$	$(-0.76 \pm 0.03) \times 10^{-1}$
$m_{\rho'}$	1603.5 ± 3.1 MeV	1564.8 ± 1.5 MeV	1636.1 ± 7.0 MeV	1600.5 ± 1.6 MeV	1482.3 ± 5.1 MeV	1552.5 ± 6.7 MeV
$\Gamma_{\rho'}$	426 ± 5 MeV	426 ± 7 MeV	611 ± 9 MeV	405 ± 8 MeV	313 ± 9 MeV	356 ± 10 MeV
$\mathrm{Re}[c_{\rho'}]$	0.30 ± 0.00	0.65 ± 0.01	1.85 ± 0.02	0.36 ± 0.01	0.49 ± 0.01	0.26 ± 0.01
$\mathrm{Im}[c_{\rho'}]$	0.31 ± 0.01	0.31 ± 0.01	0.25 ± 0.01	0.40 ± 0.01	0.27 ± 0.01	0.34 ± 0.02
$m_{\rho''}$	1899.4 ± 6.2 MeV	$1730^\dagger$ MeV	$1730^\dagger$ MeV	$1730^\dagger$ MeV	1822.2 ± 4.0 MeV	1896.2 ± 3.9 MeV
$\Gamma_{\rho''}$	406 ± 9 MeV	$260^\dagger$ MeV	$260^\dagger$ MeV	$260^\dagger$ MeV	125 ± 10 MeV	239 ± 11 MeV
$\mathrm{Re}[c_{\rho''}]$	-0.11 ± 0.00	-0.28 ± 0.00	-1.00 ± 0.04	-0.18 ± 0.01	$(-0.13 \pm 0.11) \times 10^{-1}$	$(0.78 \pm 0.14) \times 10^{-1}$
$\mathrm{Im}[c_{\rho''}]$	-0.35 ± 0.01	-0.32 ± 0.01	-0.29 ± 0.01	-0.31 ± 0.01	-0.25 ± 0.01	-0.31 ± 0.02

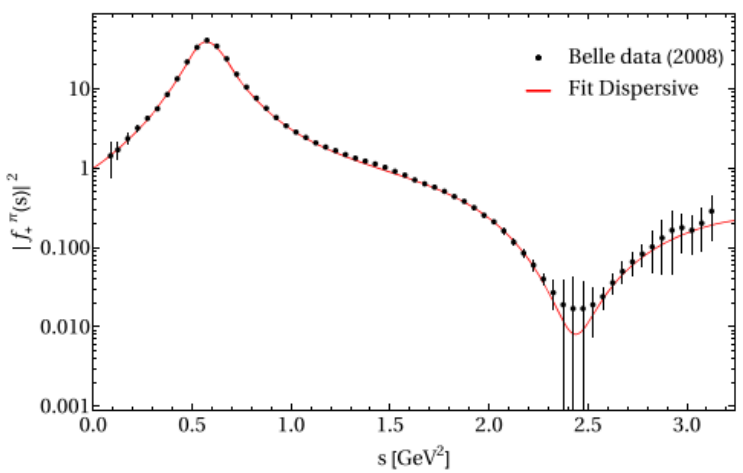
Belle data (2008)
Fit Dispersive
$|f_+^\pi(s)|^2$
s [GeV^2]

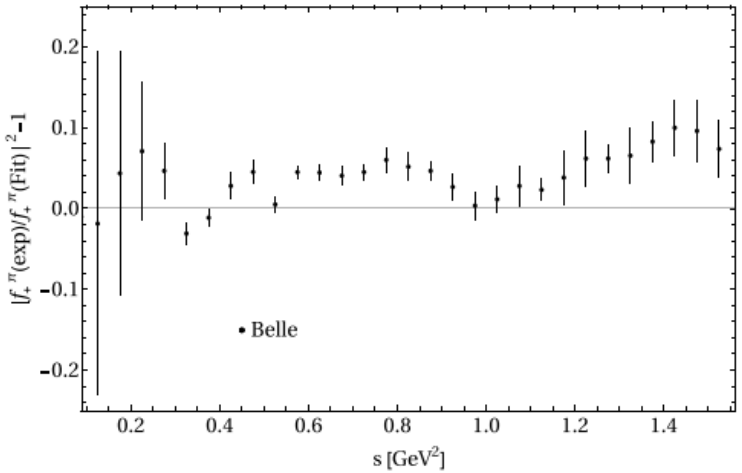
$|f_+^\pi(\text{exp})/f_+^\pi(\text{Fit})|^2-1$
Belle
s [GeV^2]

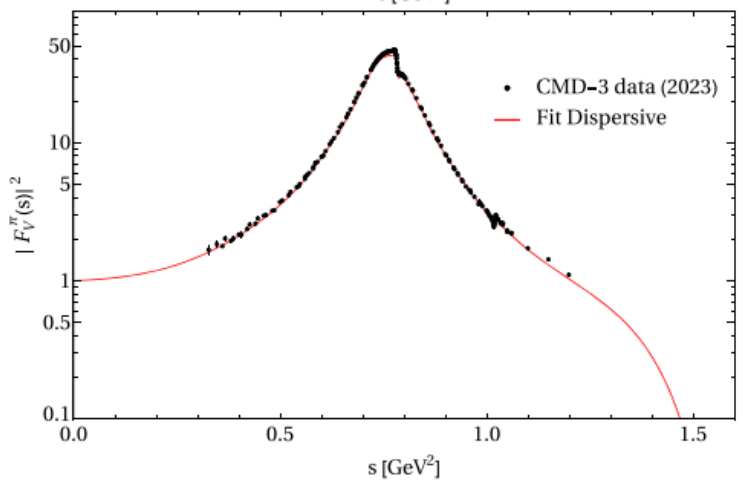
CMD–3 data (2023)
Fit Dispersive
$|F_V^\pi(s)|^2$
s [GeV^2]

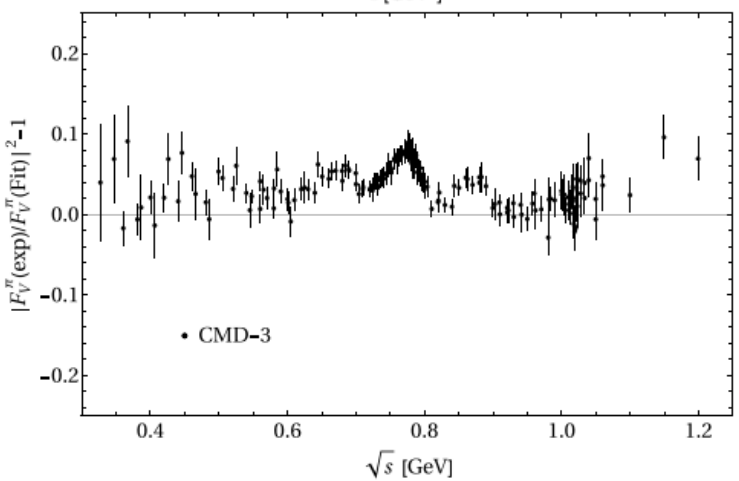
$|F_V^\pi(\text{exp})/F_V^\pi(\text{Fit})|^2-1$
CMD–3
$\sqrt{s}$ [GeV]

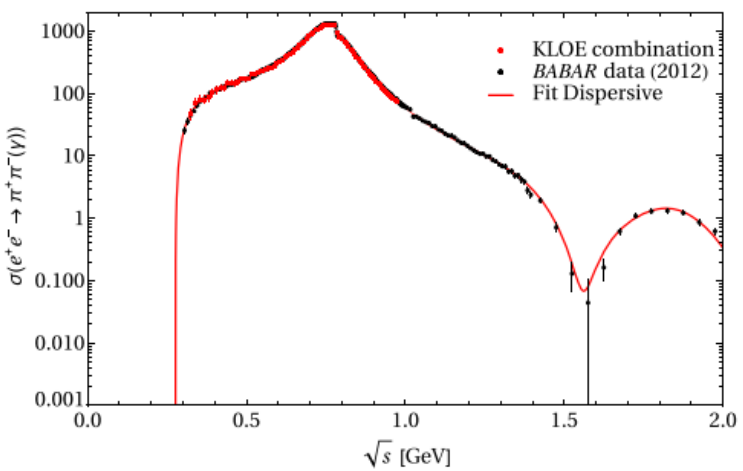
KLOE combination
BABAR data (2012)
Fit Dispersive
$\sigma(e^+e^-\to\pi^+\pi^-(\gamma))$
$\sqrt{s}$ [GeV]

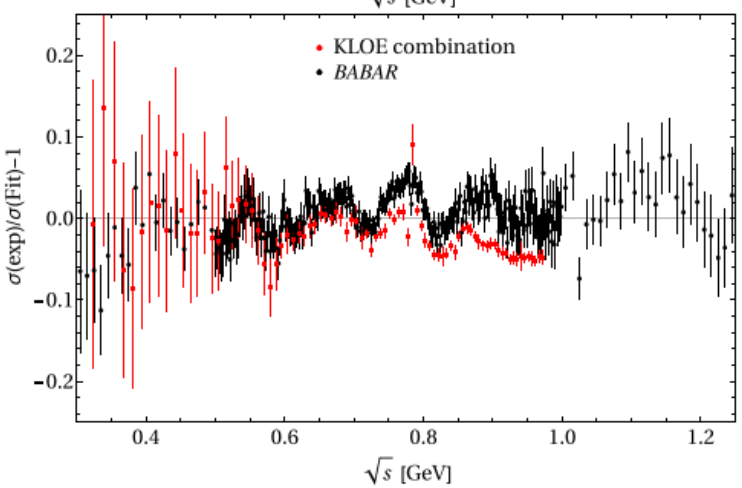
KLOE combination
BABAR
$\sigma(\text{exp})/\sigma(\text{Fit})-1$
$\sqrt{s}$ [GeV]

IB corrections to a_μ

- Contributions to a_μ from the **isospin-breaking corrections**.

	$\Delta a_\mu^{\mathrm{HVP,LO}}[\pi\pi,\tau](10^{-10})$				
	GS	KS	GP	Seed	Dispersive
Source					p_{4-1}
S_{EW}			$-12.16(0.15)$		
G_{EM}			$-1.67\binom{0.60}{1.39}$		
FSR			$+4.62(0.46)$		
$m_{\pi^\pm} - m_{\pi^0}$ effect on σ			-7.52		
$m_{\pi^\pm} - m_{\pi^0}$ effect on Γ	$+3.75$	$+4.13$	$+4.11$	$+4.15$	$+3.59$
$m_{K^\pm} - m_{K^0}$ effect on Γ	$\cdots$	$\cdots$	$+0.37$	$+0.37$	-0.22
$m_{\rho^\pm} - m_{\rho^0}$ on Γ_ρ	$\cdots$	$\cdots$	$+2.18\binom{1.97}{1.96}$	$+2.18\binom{1.98}{1.96}$	$+1.72(1.54)$
$m_{\rho^\pm} - m_{\rho^0}$	$+0.14\binom{0.22}{0.13}$	$-0.01\binom{0.08}{0.00}$	$-0.49\binom{0.44}{0.35}$	$-0.50\binom{0.45}{0.36}$	$+0.23\binom{0.23}{0.20}$
$\rho - \omega$ interference	$+3.87(0.08)$	$+4.03(0.08)$	$+4.35(0.07)$	$+3.60(0.07)$	$+2.75(0.08)$
$\rho - \phi$ interference	$+0.09(0.03)$	$+0.03(0.03)$	$\cdots$	$+0.13(0.03)$	$+0.12(0.02)$
$\pi\pi\gamma$	$-5.96(0.66)$	$-6.49(0.72)$	$-6.22(0.69)$	$-6.25(0.69)$	$-6.66(0.73)$
Total	$-14.84\binom{1.04}{1.62}$	$-15.04\binom{1.06}{1.64}$	$-12.43\binom{2.27}{2.57}$	$-13.05\binom{2.28}{2.57}$	$-15.20\binom{1.89}{2.26}\binom{0.14}{0.22}$

IB corrections to a_μ

- **Summary** of the different classes of IB corrections contributing to $\Delta a_\mu^{\text{HVP, LO}}$ **[ππ, τ]** (in units of 10^{-10}).

		Refs. [166, 194]	Ref. [209]	Refs. [237, 247]	Our estimate
Phase space		−7.88	−7.52	–	−7.7(2)
S_{EW}		−12.21(15)	−12.16(15)	–	−12.2(1.3)
G_{EM}		−1.92(90)	$(-1.67)^{+0.60}_{-1.39}$	–	−2.0(1.4)
FSR		4.67(47)	4.62(46)	4.42(4)	4.5(3)
ρ–ω mixing		4.0(4)	2.87(8)	3.79(19)	3.9(3)
$\frac{F_\pi^V}{f_+}$ (w/o ρ–ω)	ΔM_ρ	$0.20(^{+27}_{-19})(9)$	$1.95^{+1.56}_{-1.55}$	–	
	$\Delta\Gamma_\rho(\Delta M_\pi)$	4.09(0)(7)	3.37	–	
	$\Delta\Gamma_\rho(\pi\pi\gamma)$	−5.91(59)(48)	−6.66(73)	–	
	$\Delta\Gamma_\rho(g_{\rho\pi\pi})$	–	–	–	
	Total	−1.62(65)(63)	$(-1.34)^{+1.72}_{-1.71}$	–	−1.5(4.7)
Sum		−14.9(1.9)	$(-15.20)^{+2.26}_{-2.63}$	–	−15.0(5.1)

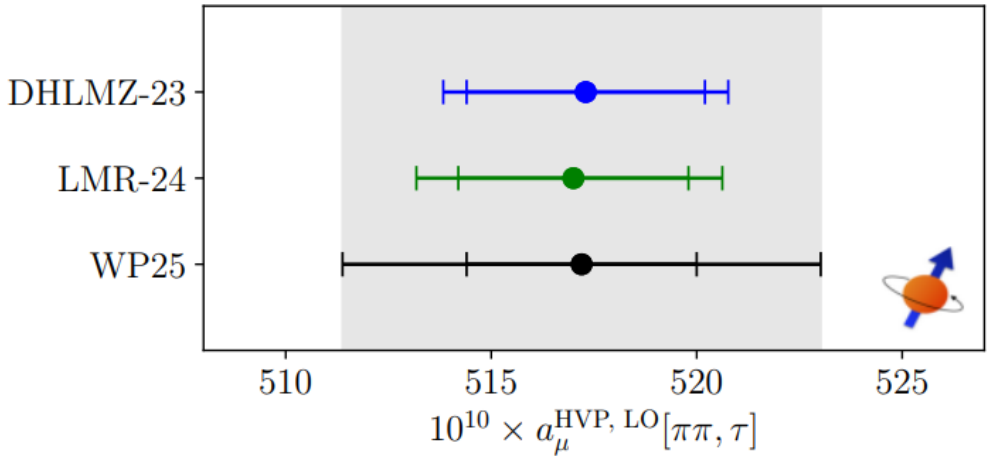

$$a_\mu^{\text{HVP, LO}}[(\pi\pi, \tau) + \text{WP20}] = 704.5(6.2) \times 10^{-10}$$

WP24 - Phys. Rept. 1143 (2025) 1-158

The Anomalous Magnetic Moment of the Muon

WP24 - Phys. Rept. 1143 (2025) 1-158

Contributions from known particles: The Standard Model

$$a_\mu(\text{SM}) = a_\mu(\text{QED}) + a_\mu(\text{Weak}) + a_\mu(\text{Hadronic})$$

QED 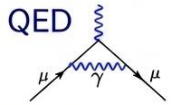 +…	$116\,584\,718.8\,(2) \times 10^{-11}$	0.002 ppm
Weak 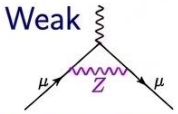 +…	$154.4\,(4) \times 10^{-11}$	0.003 ppm
Hadronic…		
…Vacuum Polarization (HVP) α^2 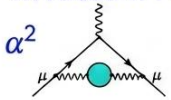 +…	$7045\,(61) \times 10^{-11}$ [0.87%]	0.52 ppm
…Light-by-Light (HLbL) α^3 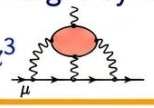 +…	$115.5\,(9.9) \times 10^{-11}$ [8.6%]	0.08 ppm

Numbers from Theory Initiative Whitepaper

Uncertainty dominated by hadronic contributions

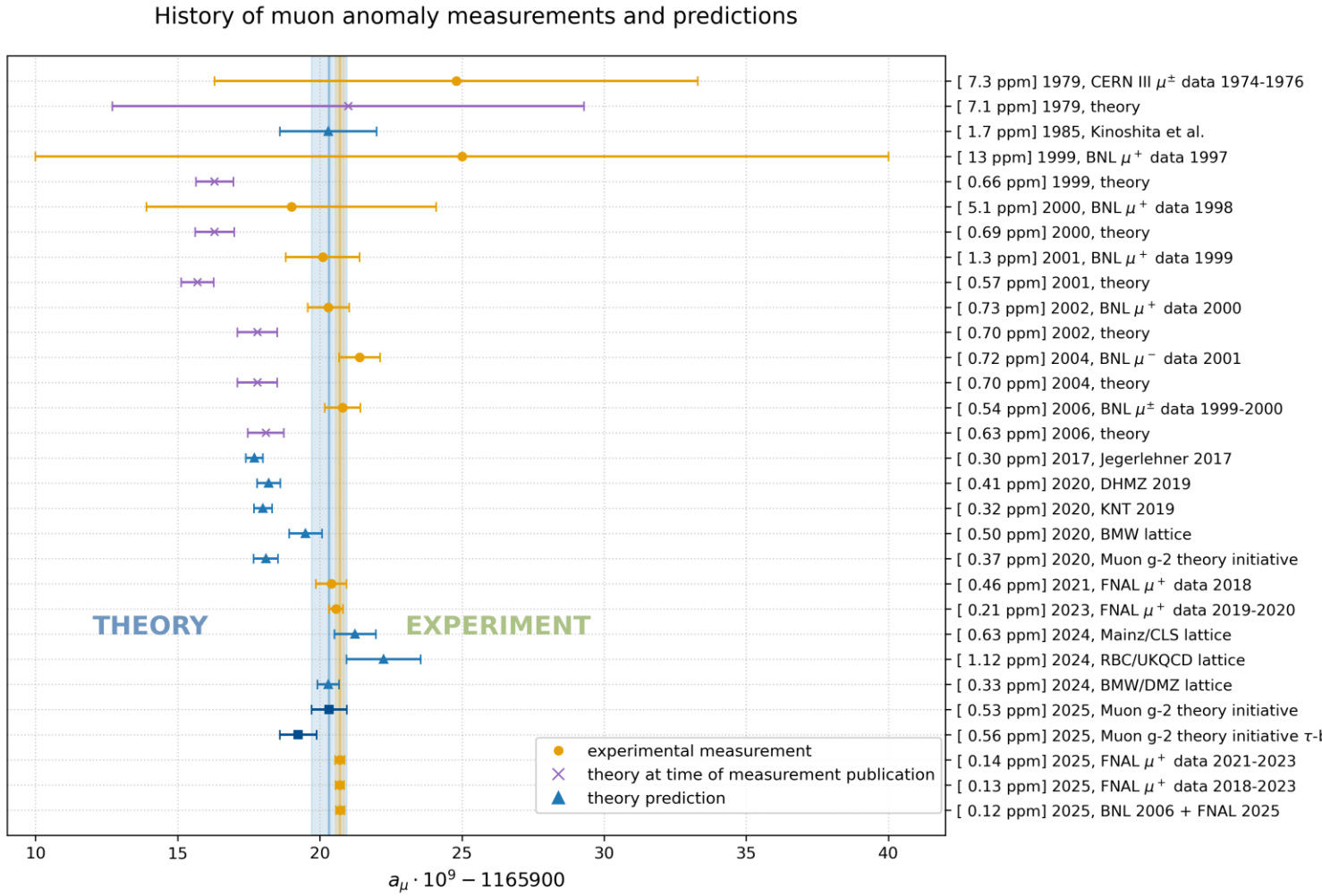

Conclusions

- There is a **global effort** in improving the **hadronic contributions** to a_μ. Specifically, dedicated studies to improve the **HVP** part from **lattice**, **dispersion relations** and **improved e^+e^- data** and **Monte Carlos** are being undertaken.
- Through the years, the **tau** data-driven estimation has always been approximately **[2,2.5]σ** away from the **experimental average**.
- The most recent **lattice** results (**Mainz/CLS, ETMC, RBC/UKQCD,…**) **agree** remarkably with **BMWc** in the **intermediate** window.
- We show that **tau based** results are **compatible** with the **lattice** evaluations in the intermediate window, being the **e^+e^- based** values in **tension** with both of them. This difference should be further scrutinized.
- In light of the puzzling situation regarding the **IB-breaking corrections** in the **tau-based** method, there is a significant effort in the **lattice** in this regard.

References

- V. Cirigliano, G. Ecker and H. Neufeld, "Radiative tau decay and the magnetic moment of the muon", JHEP 0208, 002 (2002). e-Print: hep-ph/0207310 [hep-ph]
- A. Miranda and P. Roig. "New τ -based evaluation of the hadronic contribution to the vacuum polarization piece of the muon anomalous magnetic moment". Phys.Rev.D 102 (2020) 114017. e-Print: 2007.11019 [hep-ph]
- G. Colangelo et al. "Data-driven evaluations of Euclidean windows to scrutinize hadronic vacuum polarization". Published in: Phys.Lett.B 833 (2022) 137313. e-Print: 2205.12963 [hep-ph]
- P. Masjuan, A. Miranda and P. Roig. "τ data-driven evaluation of Euclidean windows for the hadronic vacuum polarization". Published in: Phys.Lett.B 850 (2024) 138492. e-Print: 2305.20005 [hep-ph]
- López Castro, A. Miranda and P. Roig. "Isospin breaking corrections in 2π production in tau decays and e+e- annihilation: Consequences for the muon g-2 and conserved vector current tests". Published in:
- Phys.Rev.D 111 (2025) 7, 073004. e-Print: 2411.07696 [hep-ph]

Contributions at $O(p^4)$

- At $O(p^4)$ in χPT with resonances (RχT), the diagrams that contribute to these decays are:

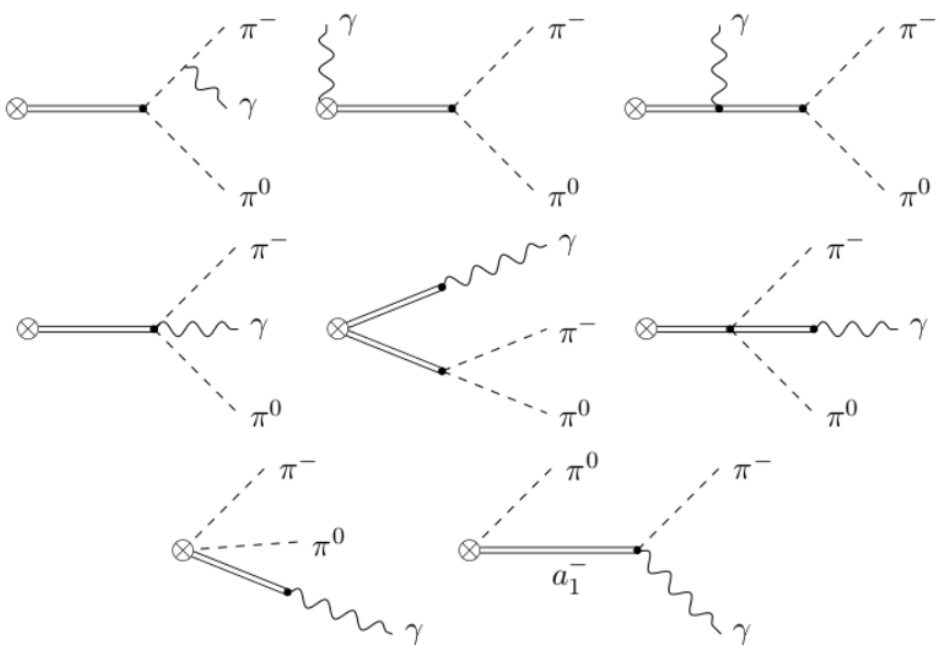

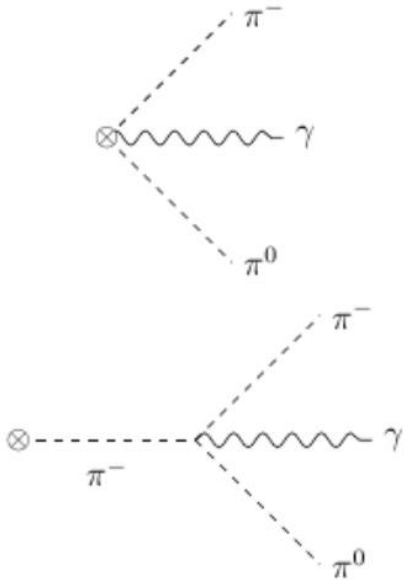

JHEP 08 (2002) 002

Contributions at $O(p^6)$

- Using the basis given by Cirigliano et al. **Nucl. Phys. B753 (2006)** and Kampf & Novotný, **Phys. Rev. D84 (2011)**, we get the following contributions at $O(p^6)$:

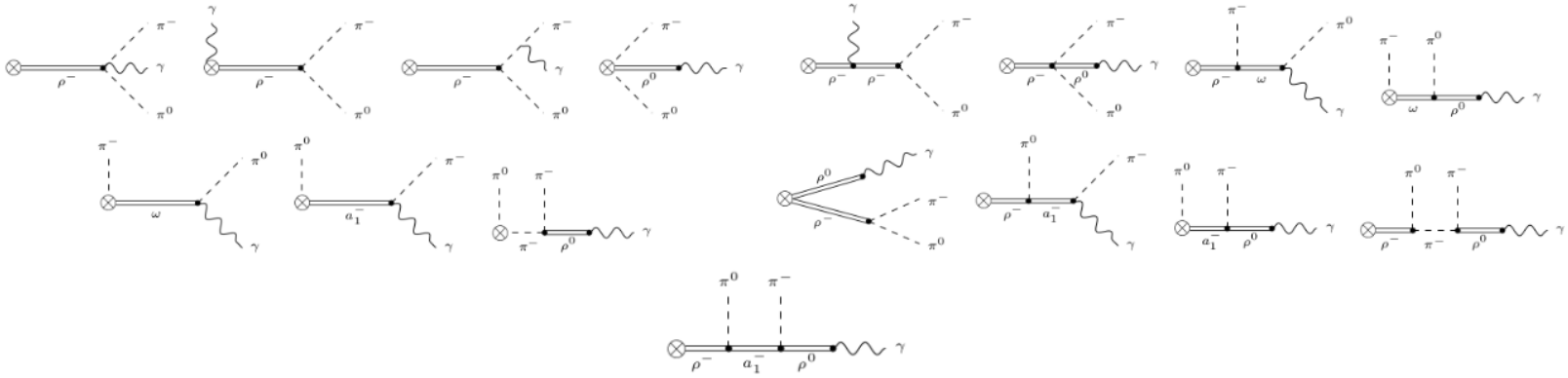

for $V_{\mu\nu}$, and

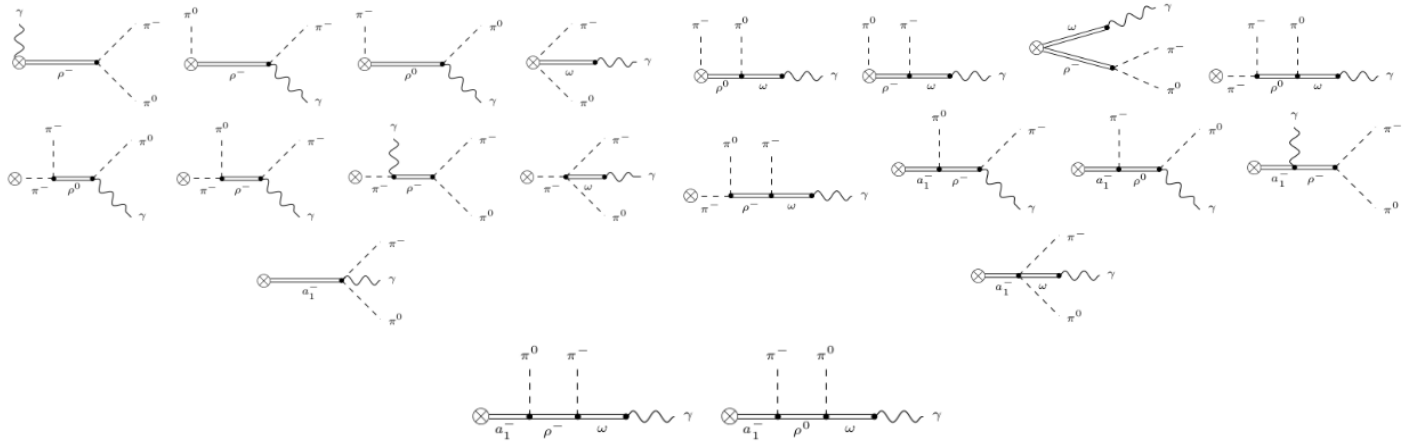

for $A_{\mu\nu}$.

Phys. Rev. D 102 (2020) 114017

HVP, LO from lattice QCD

- Comparison of recent results for the leading-order, hadronic vacuum polarization contribution to the anomalous magnetic moment of the muon:

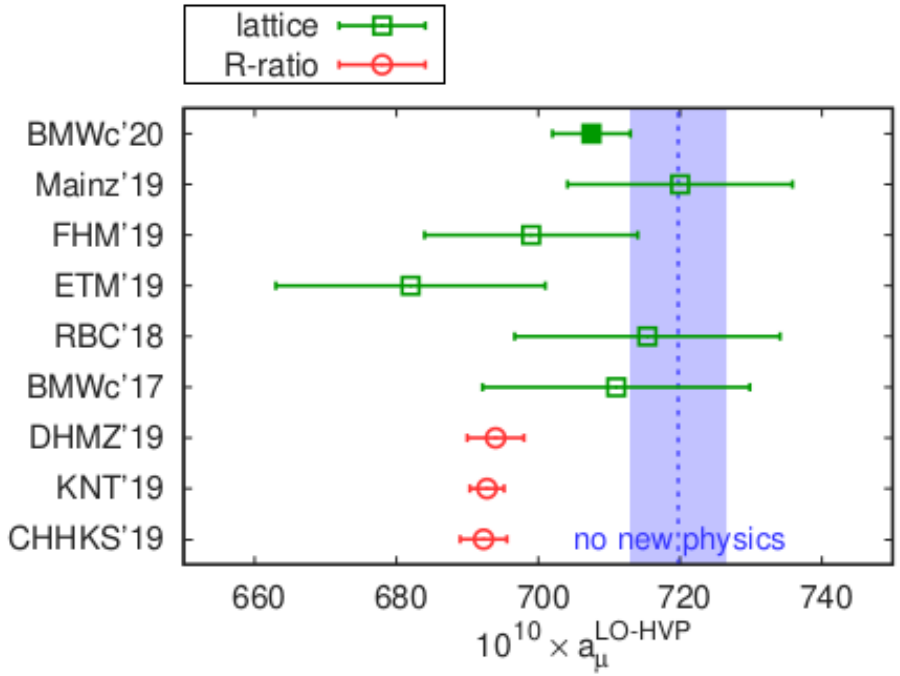

Nature (2021)

τ vs e^+e^-

- The measured branching fractions for $\tau^- \to \pi^-\pi^0 \nu_\tau$ compared to the predictions from the $e^+ e^- \to \pi^+\pi^-$ spectral functions, applying the IB corrections.

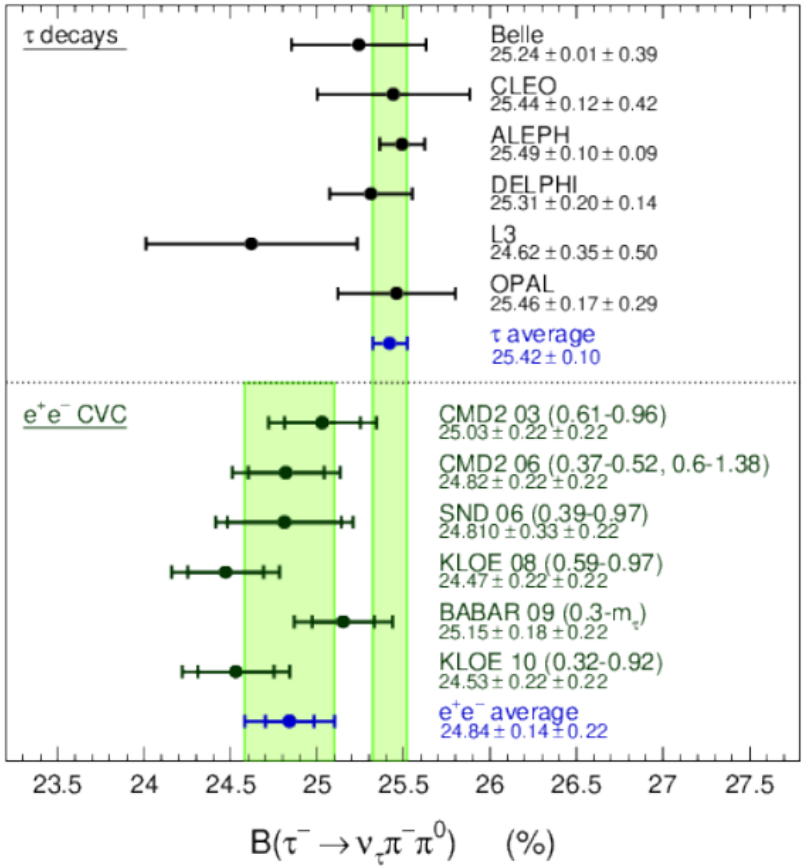

Eur.Phys.J.C66:127-136,2010

HVP, LO from e^+e^- data

- Comparison of results for the HVP, LO, evaluated between 0.6 GeV and 0.88 GeV .

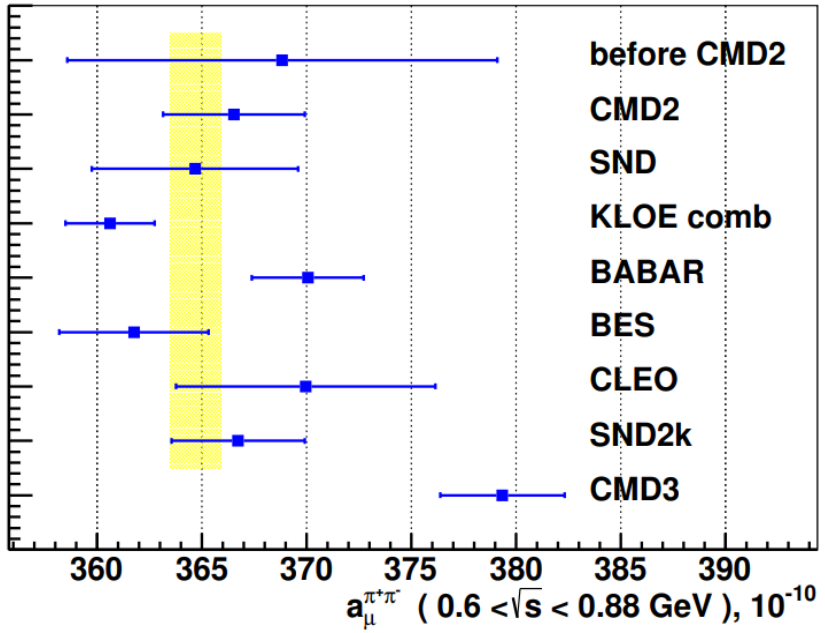

Experiment	$a_\mu^{\pi^+\pi^-,LO}, 10^{-10}$
before CMD2	368.8 ± 10.3
CMD2	366.5 ± 3.4
SND	364.7 ± 4.9
KLOE	360.6 ± 2.1
BABAR	370.1 ± 2.7
BES	361.8 ± 3.6
CLEO	370.0 ± 6.2
SND2k	366.7 ± 3.2
CMD3	379.3 ± 3.0

CMD-3. 2302.08834 [hep-ex]

$\rho-\gamma$ mixing

- $\rho-\gamma$ mixing corrections proposed in Eur.Phys.J.C71:1632,2011.

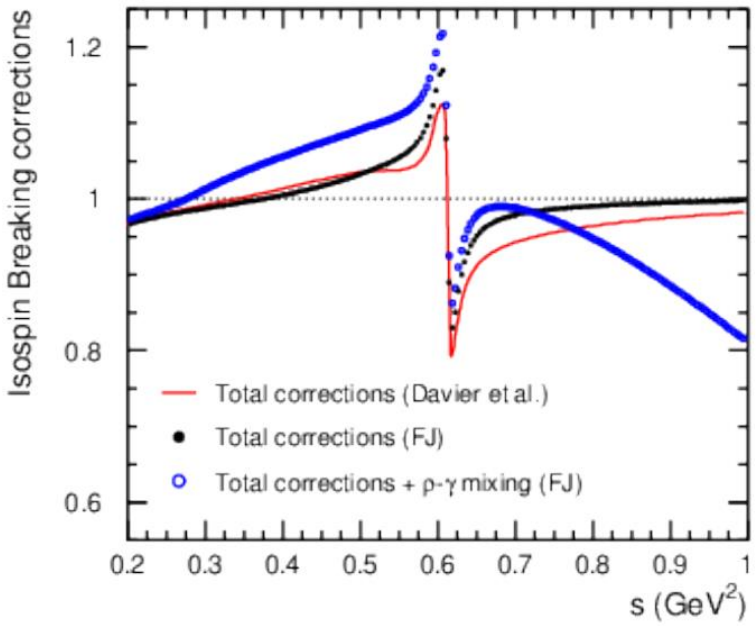

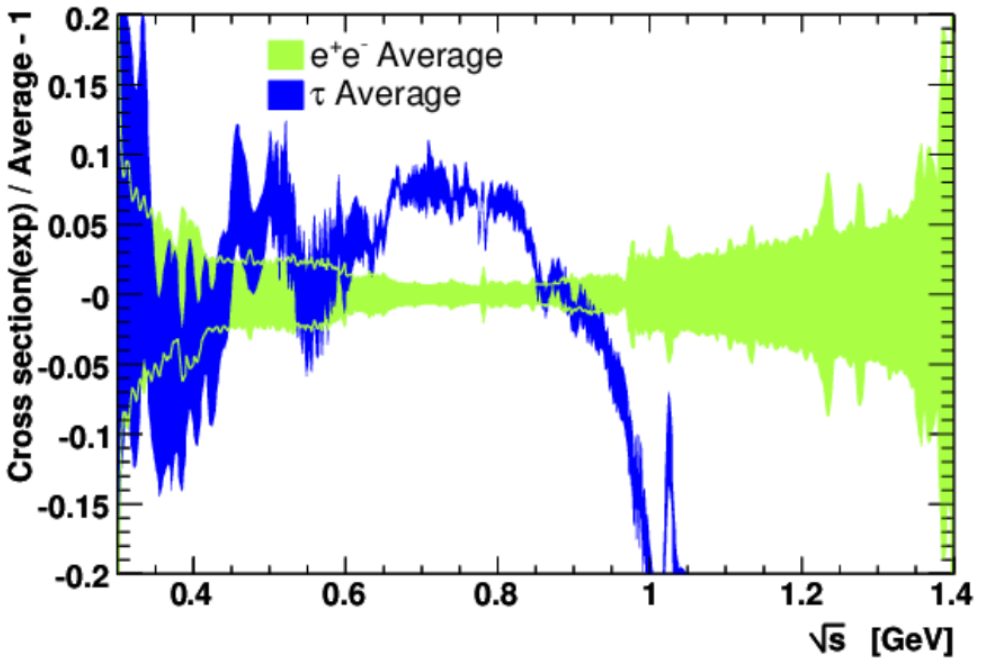

Euclidean windows

- Smoothly divide integral in several parts

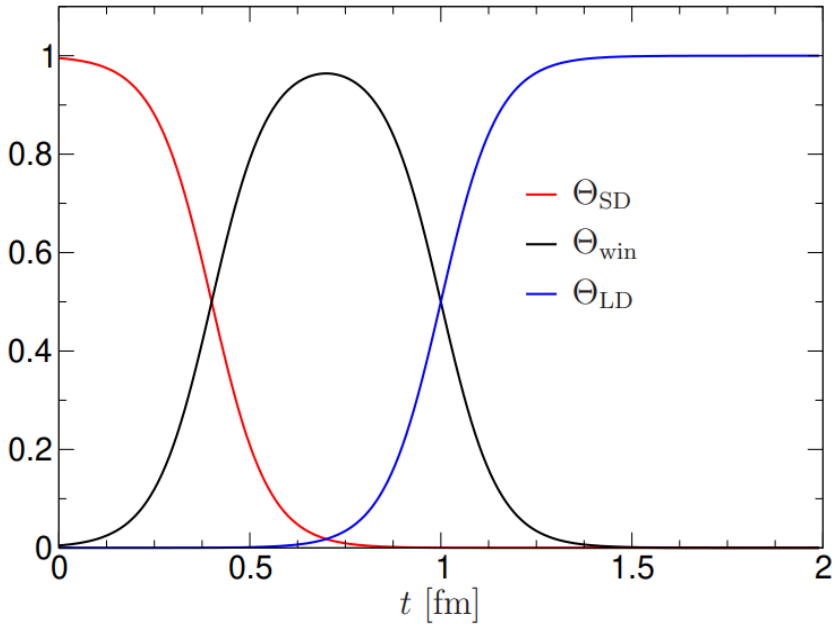

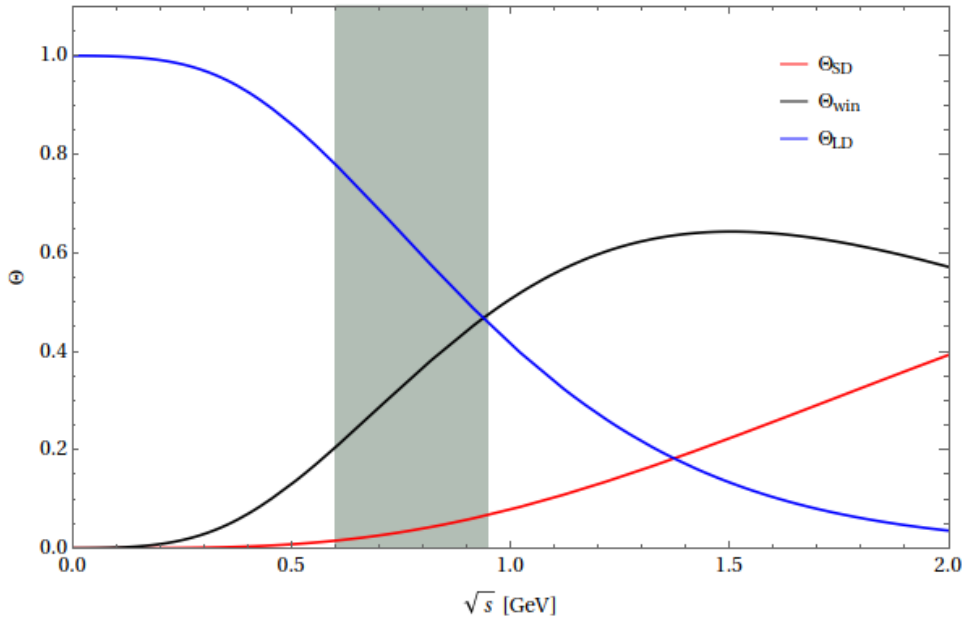

Phys.Lett.B 833 (2022) 137313

- Short-distance → cutoff effects
- Long-distance → Monte-Carlo noise
- Intermediate window: accessible with current resources
  - **Precision of 0.4 - 0.6 %**

Mattia Bruno. HADRON2023, June 5th 2023

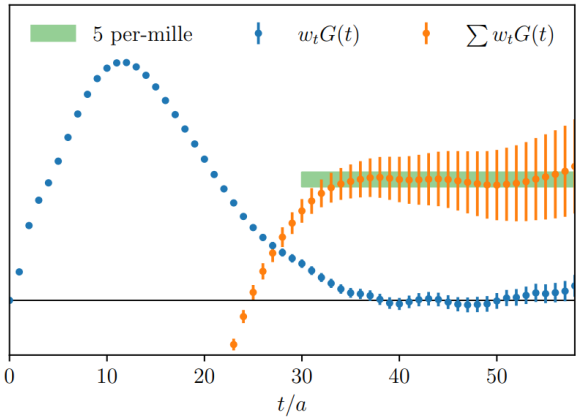

Form factor

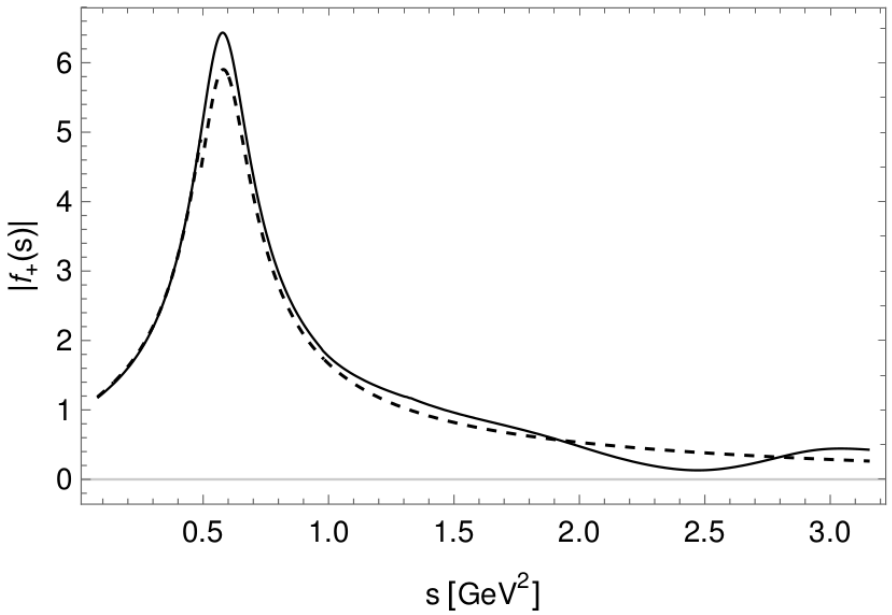
$|f_+(s)|$
0
1
2
3
4
5
6
0.5
1.0
1.5
2.0
2.5
3.0
s [GeV^2]

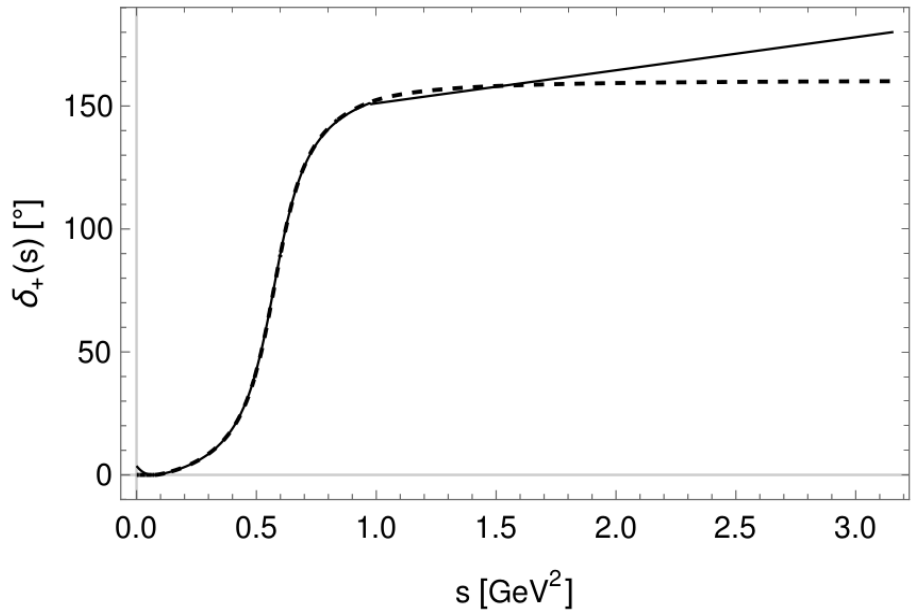
$\delta_+(s)$ [°]
0
50
100
150
0.0
0.5
1.0
1.5
2.0
2.5
3.0
s [GeV^2]

Overall IB corrections

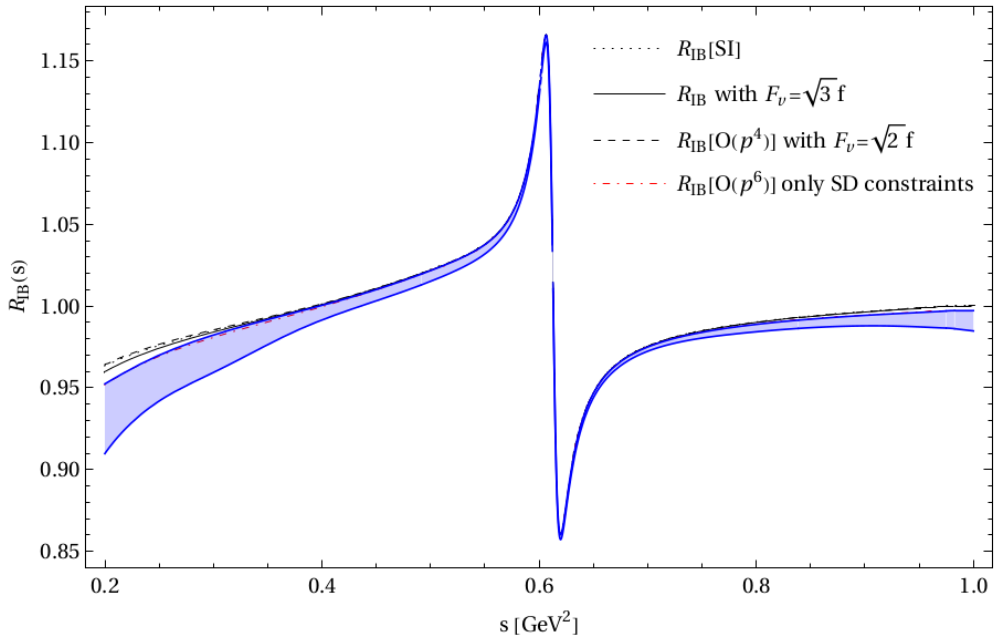

Short-distance constraints

- Using the relations for 2-point Green functions at $O(p^4)$, we have:

$$F_V = \sqrt{2}F \quad G_V = \frac{F}{\sqrt{2}} \quad F_A = F.$$

- Using the relations for 2 and 3-point Green functions at $O(p^6)$, we have:

$$F_V = \sqrt{3}F \quad G_V = \frac{F}{\sqrt{3}} \quad F_A = \sqrt{2}F.$$

Short-distance constraints

- For the parameters contributing to the leading-order chiral LECs:

$$F_V G_V = F^2, \qquad F_V^2 - F_A^2 = F^2,$$
$$F_V^2 M_V^2 = F_A^2 M_A^2, \qquad 4c_d c_m = F^2,$$
$$8\left(c_m^2 - d_m^2\right) = F^2, \qquad c_m = c_d = \sqrt{2} d_m = F/2.$$

- For the even-intrinsic parity sector:

$$\lambda_{13}^P = 0, \quad \lambda_{17}^S = \lambda_{18}^S = 0,$$
$$\lambda_{17}^A = 0, \quad \lambda_{21}^V = \lambda_{22}^V = 0.$$

- The analysis of the <VAS> Green function yields:

$$\kappa_2^S = \kappa_{14}^A = 0, \quad \kappa_4^V = 2\kappa_{15}^V, \quad \kappa_6^{VA} = \frac{F^2}{32 F_A F_V},$$
$$F_V\left(2\kappa_1^{SV} + \kappa_2^{SV}\right) = 2F_A \kappa_1^{SA} = \frac{F^2}{16\sqrt{2} c_m}.$$

Form factors

- Now let us analyze in more detail the **IB effects** in the **form factors**.
- These **IB breaking corrections** were studied by **Davier et al '09** using the **Gounaris-Sakurai** (GS) and **Kühn-Santamaria** (KS) parametrization.

$$R_{IB}(s) = \frac{FSR(s)}{G_{EM}(s)} \frac{\beta^3_{\pi^+\pi^-}}{\beta^3_{\pi^0\pi^-}} \left| \frac{F_V(s)}{f_+(s)} \right|^2,$$

$$F_\pi(s) = \frac{1}{1 + c_{\rho'} + c_{\rho''}} \left(BW^{GS}_\rho(s, m_\rho, \Gamma_\rho) \left(1 + \delta_{\rho\omega} \frac{s}{m^2} BW^{KS}_\omega(s, m_\omega, \Gamma_\omega)\right) + c_{\rho'} BW^{GS}_{\rho'}(s, m_{\rho'}, \Gamma_{\rho'}) + c_{\rho''} BW^{GS}_{\rho''}(s, m_{\rho''}, \Gamma_{\rho''}) \right),$$

$$BW^{GS}(s, m, \Gamma) = \frac{m^2 \left[1 + d(m)\Gamma/m\right]}{m^2 - s + f(s, m, \Gamma) - im\Gamma(s, m, \Gamma)},$$

$$BW^{KS}(s, m, \Gamma) = \frac{m^2}{m^2 - s - im\Gamma(s, m, \Gamma)}$$

- The **Guerrero-Pich** (GP) parametrization was employed by **Cirigliano et al '02** .

$$F_V(t) = \frac{m^2_{\rho^0}}{m^2_{\rho^0} - t - i m_{\rho^0} \Gamma_{\rho^0}(t)} \left\{ \exp\left[2\tilde{H}_{\pi^+\pi^-}(t) + \tilde{H}_{K^+K^-}(t)\right] - \frac{\theta_{\rho\omega}}{3m^2_{\rho^0}} \frac{t}{m^2_\omega - t - i\, m_\omega\, \Gamma_\omega} \right\}$$

Θρω is a real mixing parameter

$$f_+(t) = \frac{m^2_{\rho^+}}{m^2_{\rho^+} - t - i m_{\rho^+} \Gamma_{\rho^+}(t)} \exp\left\{2\tilde{H}_{\pi^+\pi^0}(t) + \tilde{H}_{K^+K^0}(t)\right\} + f^{\rm elm}_{\rm local} + \cdots,$$

Form factors

- We perform a fit using the **e+e-** and **tau** data in the **isospin-limit** including the **rho-omega mixing**.

$$\chi^2 = \sum_k^{\text{KLOE}} \left(\frac{\sigma_k^{\text{th}}(e^+e^- \to \pi^+\pi^-(\gamma)) - \sigma_k^{\text{exp}}(e^+e^- \to \pi^+\pi^-(\gamma))}{\delta\sigma_k^{\text{exp}}(e^+e^- \to \pi^+\pi^-(\gamma))} \right)^2 + \sum_k^{\text{CMD}-3} \left(\frac{|F_0^{\pi,\text{th}}|_k^2 - |F_0^{\pi,\text{exp}}|_k^2}{\delta|F_0^{\pi,\text{exp}}|_k^2} \right)^2$$
$$+ \sum_k^{\text{BABAR}} \left(\frac{\sigma_k^{\text{th}}(e^+e^- \to \pi^+\pi^-(\gamma)) - \sigma_k^{\text{exp}}(e^+e^- \to \pi^+\pi^-(\gamma))}{\delta\sigma_k^{\text{exp}}(e^+e^- \to \pi^+\pi^-(\gamma))} \right)^2 + \sum_k^{\text{Belle}} \left(\frac{|F_+^{\pi,\text{th}}|_k^2 - |F_+^{\pi,\text{exp}}|_k^2}{\delta|F_+^{\pi,\text{exp}}|_k^2} \right)^2$$

- Additionally, we consider a modification of the **GP** parametrization that includes the **rho'** and **rho''** contributions.

$$\begin{aligned} F_V(s)^{\text{seed}} &= \frac{M_\rho^2 + s(\gamma e^{i\phi_1} + \delta e^{i\phi_2})}{M_\rho^2 - s - iM_\rho\Gamma_\rho(s)} \exp\left\{ \text{Re}\left[-\frac{s}{96\pi^2 F_\pi^2} \left(A_\pi(s) + \frac{1}{2} A_K(s) \right) \right] \right\} \\ &- \gamma \frac{s e^{i\phi_1}}{M_{\rho'}^2 - s - iM_{\rho'}\Gamma_{\rho'}(s)} \exp\left\{ \frac{s\Gamma_{\rho'}(M_{\rho'}^2)}{\pi M_{\rho'}^3 \sigma_\pi^3(M_{\rho'}^2)} \text{Re}A_\pi(s) \right\} \\ &- \delta \frac{s e^{i\phi_2}}{M_{\rho''}^2 - s - iM_{\rho''}\Gamma_{\rho''}(s)} \exp\left\{ \frac{s\Gamma_{\rho''}(M_{\rho''}^2)}{\pi M_{\rho''}^3 \sigma_\pi^3(M_{\rho''}^2)} \text{Re}A_\pi(s) \right\}, \end{aligned}$$

Fit results for the GS model

	BABAR12 + Belle	KLOE12 + Belle	KLOEc + Belle	CMD3 + Belle	Global fit 1	Global fit 2
Data points	$337 + 62$	$60 + 62$	$85 + 62$	$209 + 62$	$337 + 60 + 209 + 62$	$337 + 85 + 209 + 62$
$\chi^2_{ee} + \chi^2_{\tau}$	$327.4 + 99.5$	$157.9 + 274.5$	$138.2 + 377.5$	$181.6 + 87.3$	$1686.8 + 143.4$	$2786.8 + 214.1$
χ^2	426.9	432.4	515.7	268.9	1830.2	3000.9
χ^2/d.o.f.	1.1	3.9	3.8	1.0	2.8	4.4
m_ρ	774.0 ± 0.1 MeV	773.4 ± 0.2 MeV	773.5 ± 0.1 MeV	773.4 ± 0.1 MeV	773.5 ± 0.1 MeV	772.9 ± 0.1 MeV
Γ_ρ	148.9 ± 0.3 MeV	144.7 ± 0.5 MeV	147.1 ± 0.3 MeV	147.6 ± 0.2 MeV	146.6 ± 0.2 MeV	146.9 ± 0.2 MeV
$\lvert\delta_{\rho\omega}\rvert$	$(2.1 \pm 0.0) \times 10^{-3}$	$(1.9 \pm 0.1) \times 10^{-3}$	$(1.8 \pm 0.0) \times 10^{-3}$	$(2.0 \pm 0.0) \times 10^{-3}$	$(1.9 \pm 0.0) \times 10^{-3}$	$(2.0 \pm 0.0) \times 10^{-3}$
$\arg[\delta_{\rho\omega}]$	$(10.8 \pm 1.1)°$	$(13.8 \pm 2.6)°$	$(18.2 \pm 2.6)°$	$(12.0 \pm 0.5)°$	$(10.1 \pm 0.4)°$	$(5.5 \pm 0.4)°$
$\lvert\delta_{\rho\phi}\rvert$	$0^\dagger$	$0^\dagger$	$0^\dagger$	$(2.2 \pm 0.2) \times 10^{-4}$	$(1.5 \pm 0.2) \times 10^{-4}$	$(1.4 \pm 0.2) \times 10^{-4}$
$\arg[\delta_{\rho\phi}]$	...	...	...	$(83.8 \pm 5.9)°$	$(68.4 \pm 7.8)°$	$(46.6 \pm 8.6)°$
$m_{\rho'}$	1460.9 ± 5.9 MeV	1412.9 ± 7.8 MeV	1398.9 ± 6.7 MeV	1459.0 ± 7.0 MeV	1433.3 ± 4.8 MeV	1443.7 ± 5.2 MeV
$\Gamma_{\rho'}$	444 ± 14 MeV	441 ± 20 MeV	445 ± 20 MeV	450 ± 20 MeV	403 ± 12 MeV	391 ± 11 MeV
$\mathrm{Re}[c_{\rho'}]$	-0.12 ± 0.00	-0.11 ± 0.00	-0.11 ± 0.01	-0.10 ± 0.00	-0.09 ± 0.00	-0.11 ± 0.00
$\mathrm{Im}[c_{\rho'}]$	-0.03 ± 0.01	0.03 ± 0.01	-0.26 ± 0.02	-0.20 ± 0.02	-0.17 ± 0.01	-0.02 ± 0.00
$m_{\rho''}$	1806.7 ± 9.7 MeV	$1730^\dagger$ MeV	$1730^\dagger$ MeV	$1730^\dagger$ MeV	1784.8 ± 10.5 MeV	1816.8 ± 9.2 MeV
$\Gamma_{\rho''}$	273 ± 16 MeV	$260^\dagger$ MeV	$260^\dagger$ MeV	$260^\dagger$ MeV	245 ± 14 MeV	245 ± 16 MeV
$\mathrm{Re}[c_{\rho''}]$	$(2.9 \pm 0.5) \times 10^{-2}$	$(4.9 \pm 0.6) \times 10^{-2}$	$(-7.7 \pm 0.7) \times 10^{-2}$	$(-7.5 \pm 0.6) \times 10^{-2}$	$(-6.6 \pm 0.6) \times 10^{-2}$	$(2.1 \pm 0.4) \times 10^{-2}$
$\mathrm{Im}[c_{\rho''}]$	$(4.5 \pm 0.3) \times 10^{-2}$	$(1.7 \pm 0.3) \times 10^{-2}$	$(-1.7 \pm 0.6) \times 10^{-3}$	$(5.8 \pm 6.7) \times 10^{-3}$	$(-2.9 \pm 0.4) \times 10^{-2}$	$(4.0 \pm 0.2) \times 10^{-2}$

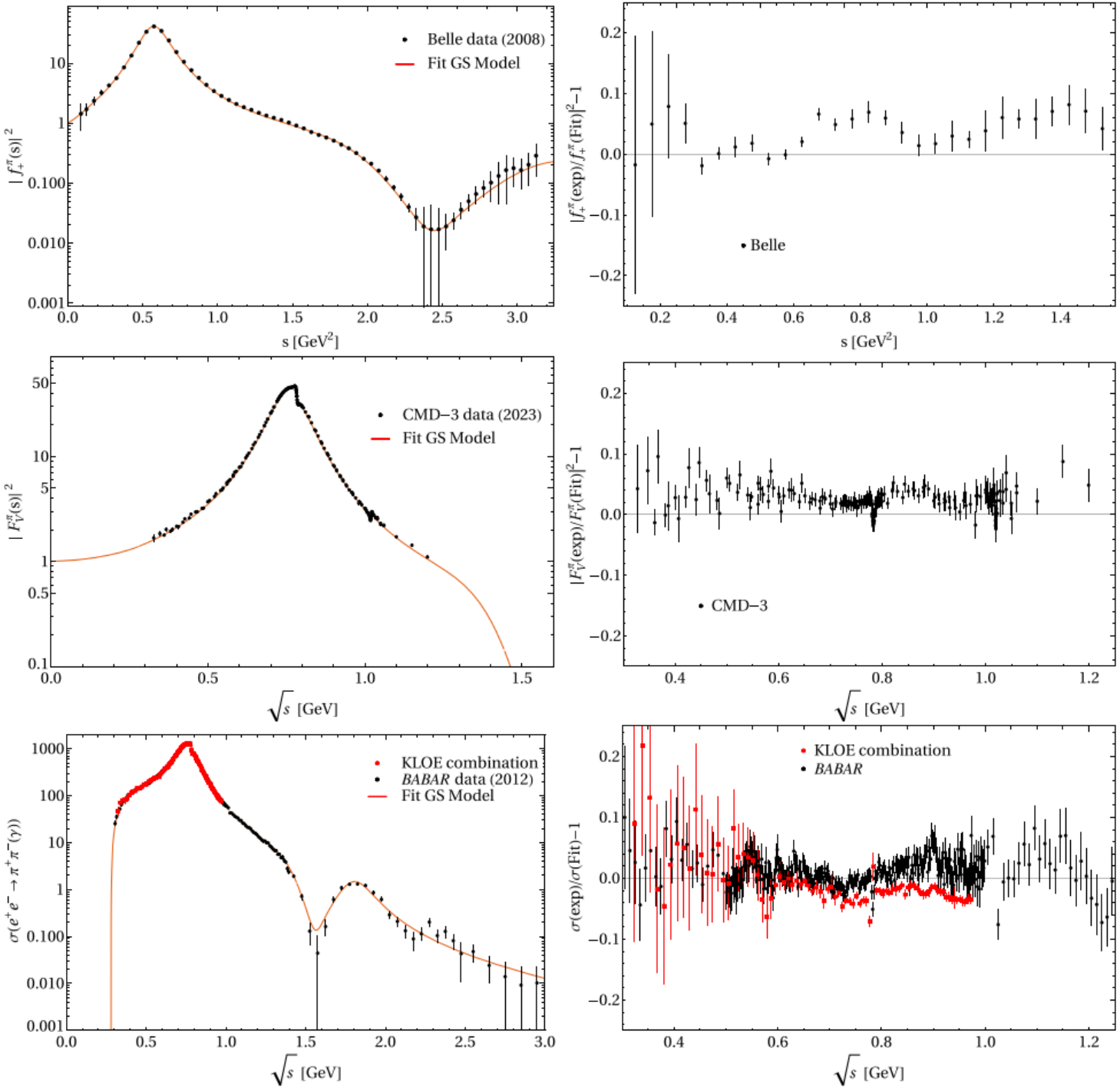
Belle data (2008)
Fit GS Model
$|f_+^\pi(s)|^2$
s [GeV^2]
$|f_+^\pi(\text{exp})/f_+^\pi(\text{Fit})|^2-1$
Belle
CMD−3 data (2023)
Fit GS Model
$|F_V^\pi(s)|^2$
$\sqrt{s}$ [GeV]
$|F_V^\pi(\text{exp})/F_V^\pi(\text{Fit})|^2-1$
CMD−3
KLOE combination
BABAR data (2012)
Fit GS Model
$\sigma(e^+e^-\to\pi^+\pi^-(\gamma))$
$\sqrt{s}$ [GeV]
KLOE combination
BABAR
$\sigma(\text{exp})/\sigma(\text{Fit})-1$
$\sqrt{s}$ [GeV]

Fit results for the KS model

	BABAR12 + Belle	KLOE12 + Belle	KLOEc + Belle	CMD3 + Belle	Global fit 1	Global fit 2
Data points	$337 + 62$	$60 + 62$	$85 + 62$	$209 + 62$	$337 + 60 + 209 + 62$	$337 + 85 + 209 + 62$
$\chi^2_{ee} + \chi^2_{\tau}$	$395.7 + 122.7$	$181.5 + 314.8$	$236.1 + 432.2$	$463.3 + 151.5$	$2070.6 + 200.0$	$3100.7 + 318.8$
χ^2	518.4	496.3	668.3	614.8	2270.6	3419.5
χ^2/d.o.f.	1.3	4.4	4.9	2.4	3.5	5.0
m_ρ	772.3 ± 0.1 MeV	771.8 ± 0.2 MeV	771.6 ± 0.1 MeV	771.4 ± 0.1 MeV	771.8 ± 0.1 MeV	771.5 ± 0.1 MeV
Γ_ρ	147.5 ± 0.3 MeV	142.5 ± 0.4 MeV	145.0 ± 0.3 MeV	146.0 ± 0.2 MeV	145.5 ± 0.2 MeV	145.7 ± 0.2 MeV
$\lvert\delta_{\rho\omega}\rvert$	$(1.9 \pm 0.0) \times 10^{-3}$	$(1.7 \pm 0.1) \times 10^{-3}$	$(1.7 \pm 0.0) \times 10^{-3}$	$(2.0 \pm 0.0) \times 10^{-3}$	$(1.9 \pm 0.0) \times 10^{-3}$	$(1.9 \pm 0.0) \times 10^{-3}$
$\arg[\delta_{\rho\omega}]$	$(11.7 \pm 1.1)°$	$(17.6 \pm 2.9)°$	$(17.6 \pm 2.7)°$	$(11.3 \pm 0.5)°$	$(9.5 \pm 0.4)°$	$(6.5 \pm 0.4)°$
$\lvert\delta_{\rho\phi}\rvert$	$0^\dagger$	$0^\dagger$	$0^\dagger$	$(2.8 \pm 0.2) \times 10^{-4}$	$(1.7 \pm 0.2) \times 10^{-4}$	$(1.4 \pm 0.2) \times 10^{-4}$
$\arg[\delta_{\rho\phi}]$	...	...	...	$(87.0 \pm 4.9)°$	$(78.9 \pm 7.5)°$	$(73.2 \pm 8.1)°$
$m_{\rho'}$	1536.1 ± 9.5 MeV	1425.2 ± 8.3 MeV	1476.7 ± 8.0 MeV	1575.8 ± 10.9 MeV	1564.9 ± 9.3 MeV	1547.5 ± 8.1 MeV
$\Gamma_{\rho'}$	538 ± 18 MeV	471 ± 18 MeV	474 ± 14 MeV	717 ± 23 MeV	450 ± 17 MeV	447 ± 16 MeV
$\mathrm{Re}[c_{\rho'}]$	-0.13 ± 0.01	-0.13 ± 0.00	-0.13 ± 0.00	-0.23 ± 0.01	$(3.6 \pm 3.3) \times 10^{-2}$	$(-0.6 \pm 2.7) \times 10^{-2}$
$\mathrm{Im}[c_{\rho'}]$	-0.28 ± 0.02	-0.19 ± 0.02	-0.17 ± 0.02	-0.23 ± 0.01	-0.28 ± 0.03	-0.27 ± 0.02
$m_{\rho''}$	1831.4 ± 12.6 MeV	$1730^\dagger$ MeV	$1730^\dagger$ MeV	$1730^\dagger$ MeV	1865.8 ± 20.1 MeV	1868.2 ± 16.3 MeV
$\Gamma_{\rho''}$	442 ± 33 MeV	$260^\dagger$ MeV	$260^\dagger$ MeV	$260^\dagger$ MeV	721 ± 53 MeV	650 ± 50 MeV
$\mathrm{Re}[c_{\rho''}]$	$-(8.4 \pm 1.5) \times 10^{-2}$	$(-6.0 \pm 0.6) \times 10^{-2}$	$(-5.0 \pm 0.7) \times 10^{-2}$	$(1.9 \pm 1.0) \times 10^{-2}$	-0.25 ± 0.04	-0.20 ± 0.03
$\mathrm{Im}[c_{\rho''}]$	0.13 ± 0.01	$(3.1 \pm 0.7) \times 10^{-2}$	$(4.6 \pm 0.7) \times 10^{-2}$	0.10 ± 0.00	0.13 ± 0.02	0.12 ± 0.01

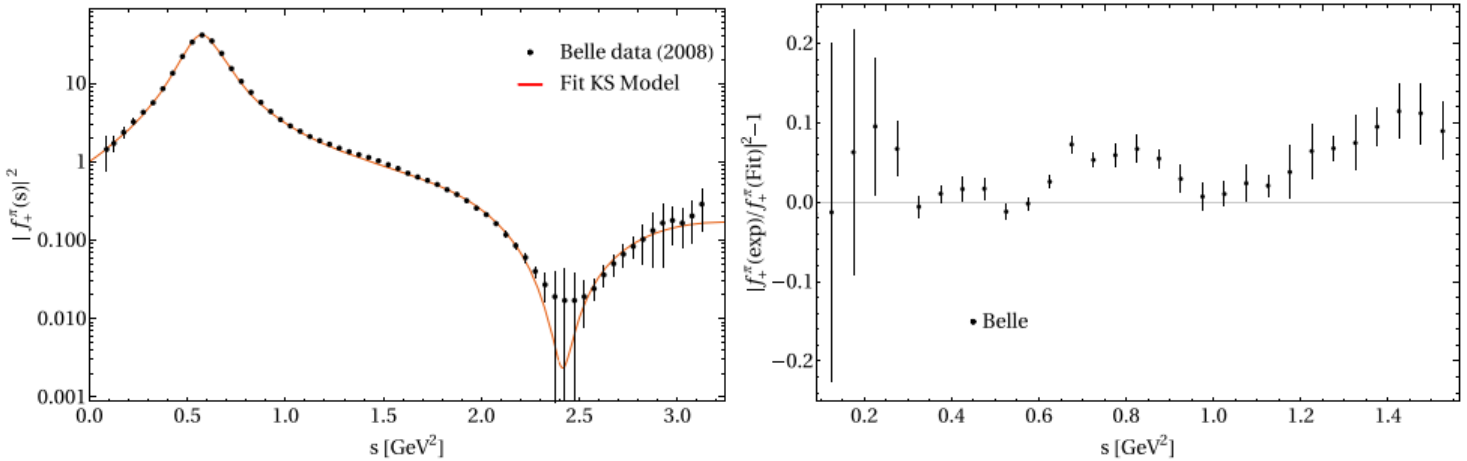
Belle data (2008)
Fit KS Model
$|f_+^\pi(s)|^2$
s [GeV^2]

Belle
$|f_+^\pi(\text{exp})/f_+^\pi(\text{Fit})|^2-1$
s [GeV^2]

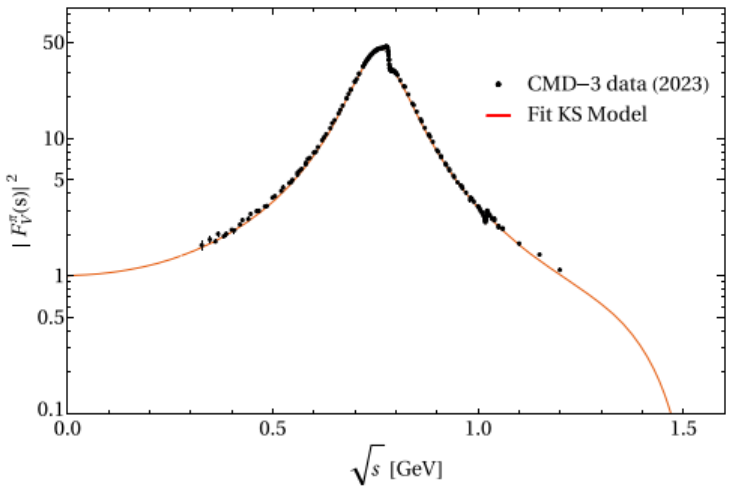
CMD−3 data (2023)
Fit KS Model
$|F_V^\pi(s)|^2$
$\sqrt{s}$ [GeV]

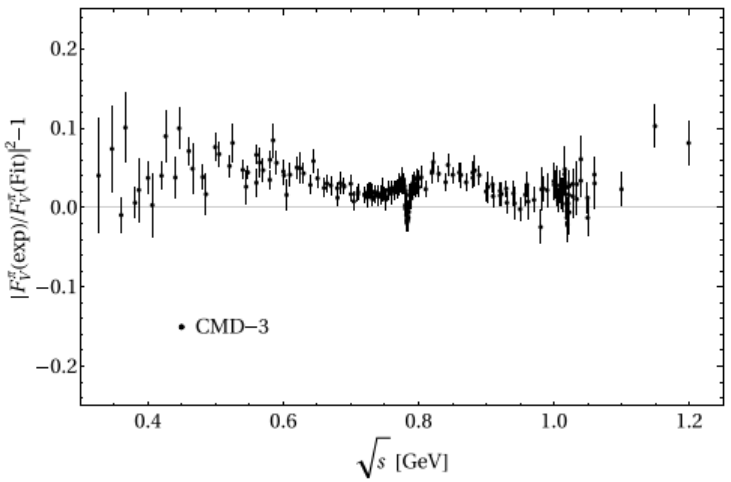
CMD−3
$|F_V^\pi(\text{exp})/F_V^\pi(\text{Fit})|^2-1$
$\sqrt{s}$ [GeV]

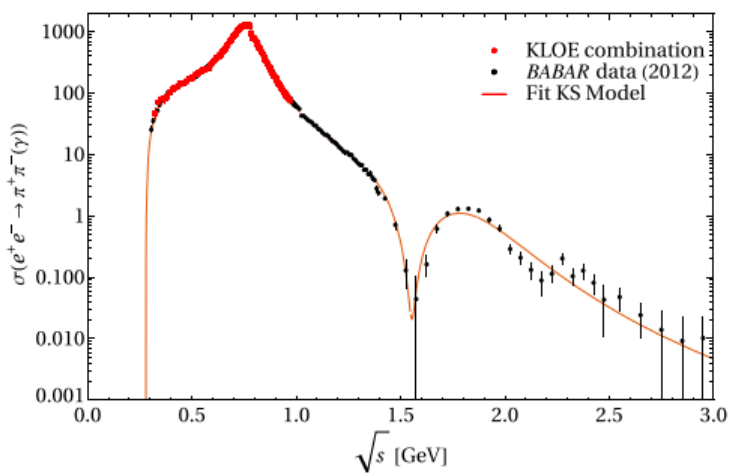
KLOE combination
BABAR data (2012)
Fit KS Model
$\sigma(e^+e^-\to\pi^+\pi^-(\gamma))$
$\sqrt{s}$ [GeV]

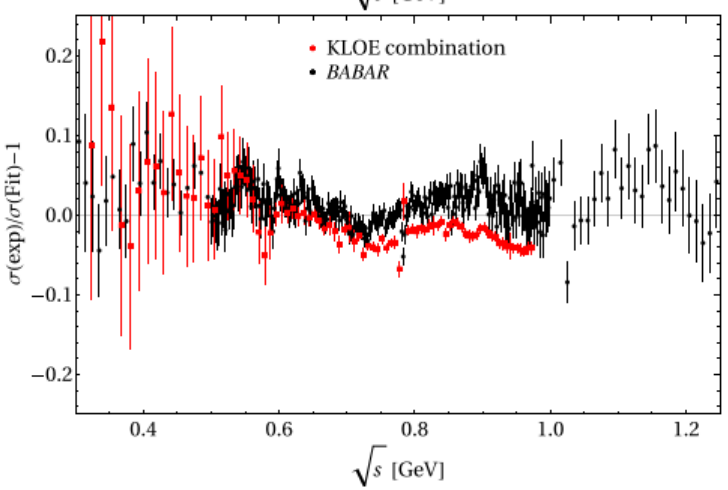
KLOE combination
BABAR
$\sigma(\text{exp})/\sigma(\text{Fit})-1$
$\sqrt{s}$ [GeV]

Fit results for the GP model

	BABAR12 + Belle	KLOE12 + Belle	KLOEc + Belle	CMD3 + Belle	Global fit 1	Global fit 2
Data points	$270 + 19$	$60 + 19$	$85 + 19$	$172 + 19$	$270 + 60 + 172 + 19$	$270 + 85 + 172 + 19$
$\chi^2_{ee} + \chi^2_{\tau}$	$1089.1 + 582.6$	$53.0 + 519.5$	$265.1 + 583.8$	$2607.9 + 671.7$	$4274.1 + 613.0$	$4444.5 + 620.9$
χ^2	1671.7	572.5	848.9	3279.6	4887.1	5065.4
χ^2/d.o.f.	5.8	7.5	8.4	17.4	9.4	9.3
m_ρ	776.0 ± 0.1 MeV	777.4 ± 0.1 MeV	776.0 ± 0.1 MeV	774.8 ± 0.1 MeV	775.5 ± 0.1 MeV	775.4 ± 0.1 MeV
$\mathrm{Re}\lvert\delta_{\rho\omega}\rvert = \mathrm{Re}\lvert -\frac{\theta_{\rho\omega}}{3m_\rho}\rvert$	$(2.5 \pm 0.0) \times 10^{-3}$	$(2.6 \pm 0.1) \times 10^{-3}$	$(2.5 \pm 0.1) \times 10^{-3}$	$(2.5 \pm 0.0) \times 10^{-3}$	$(2.5 \pm 0.0) \times 10^{-3}$	$(2.5 \pm 0.0) \times 10^{-3}$
$\mathrm{Im}\lvert\delta_{\rho\omega}\rvert = \mathrm{Im}\lvert -\frac{\theta_{\rho\omega}}{3m_\rho}\rvert$	$(0.3 \pm 0.0) \times 10^{-3}$	$(0.4 \pm 0.1) \times 10^{-3}$	$(0.8 \pm 0.1) \times 10^{-3}$	$(0.1 \pm 0.0) \times 10^{-3}$	$(0.1 \pm 0.0) \times 10^{-3}$	$(0.1 \pm 0.0) \times 10^{-3}$
$\lvert\delta_{\rho\omega}\rvert$	$(2.6 \pm 0.0) \times 10^{-3}$	$(2.6 \pm 0.1) \times 10^{-3}$	$(2.7 \pm 0.1) \times 10^{-3}$	$(2.5 \pm 0.0) \times 10^{-3}$	$(2.5 \pm 0.0) \times 10^{-3}$	$(2.5 \pm 0.0) \times 10^{-3}$
$\arg[\delta_{\rho\omega}]$	$(6.2 \pm 0.9)^\circ$	$(9.2 \pm 2.1)^\circ$	$(18.6 \pm 1.8)^\circ$	$(1.4 \pm 0.4)^\circ$	$(2.6 \pm 0.3)^\circ$	$(2.8 \pm 0.3)^\circ$

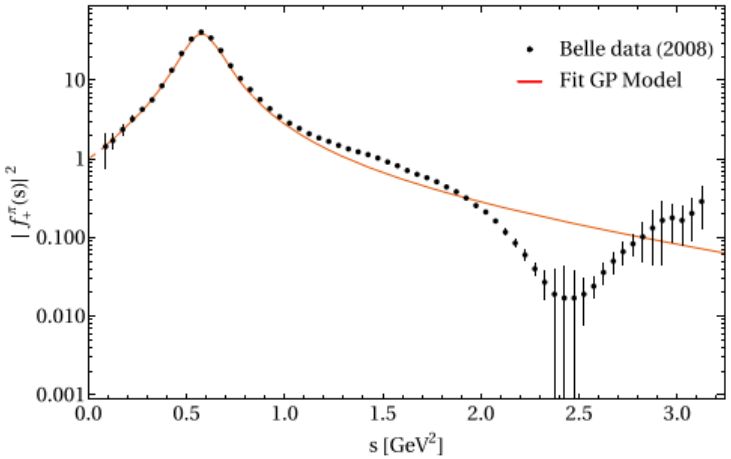
Belle data (2008)
Fit GP Model
$|f_+^\pi(s)|^2$
s [GeV^2]

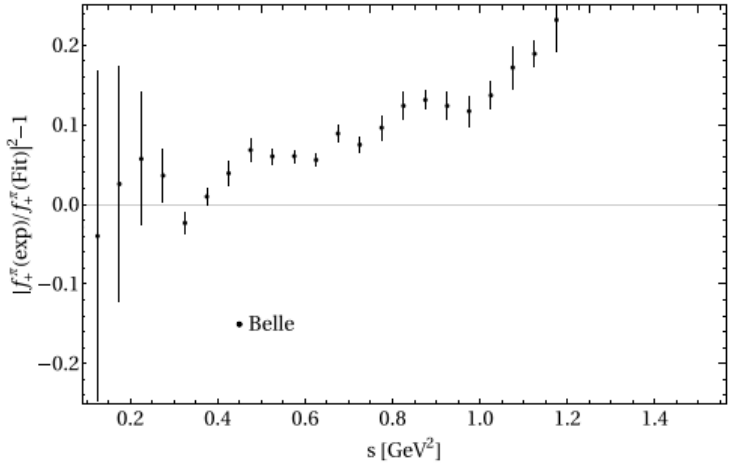
$|f_+^\pi(\text{exp})/f_+^\pi(\text{Fit})|^2-1$
Belle
s [GeV^2]

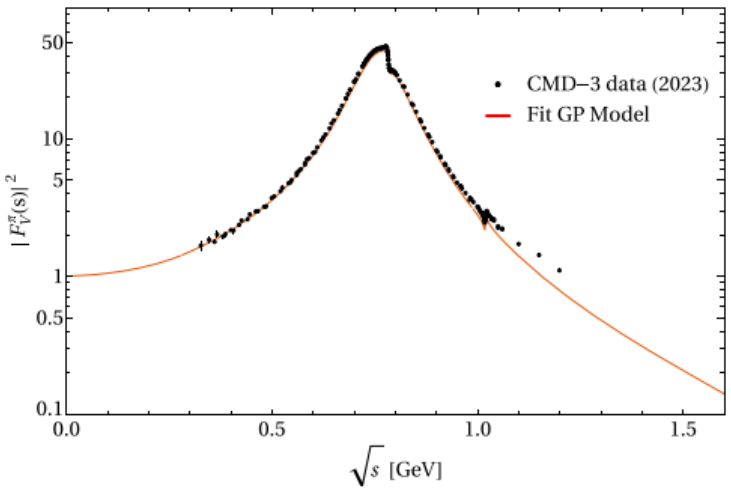
CMD−3 data (2023)
Fit GP Model
$|F_V^\pi(s)|^2$
$\sqrt{s}$ [GeV]

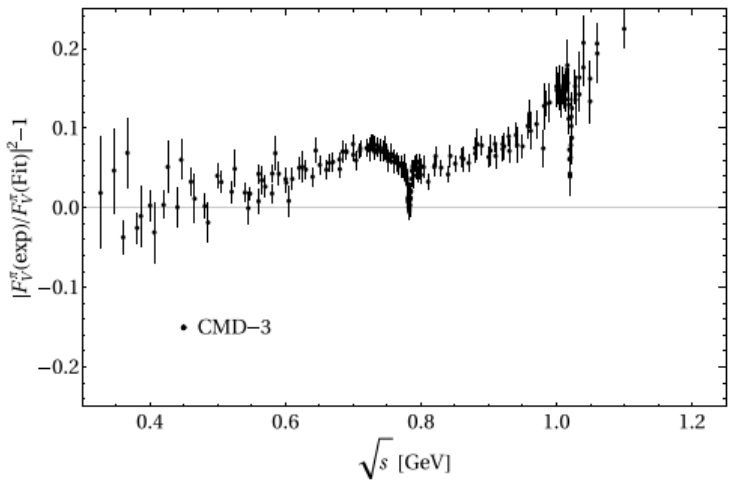
$|F_V^\pi(\text{exp})/F_V^\pi(\text{Fit})|^2-1$
CMD−3
$\sqrt{s}$ [GeV]

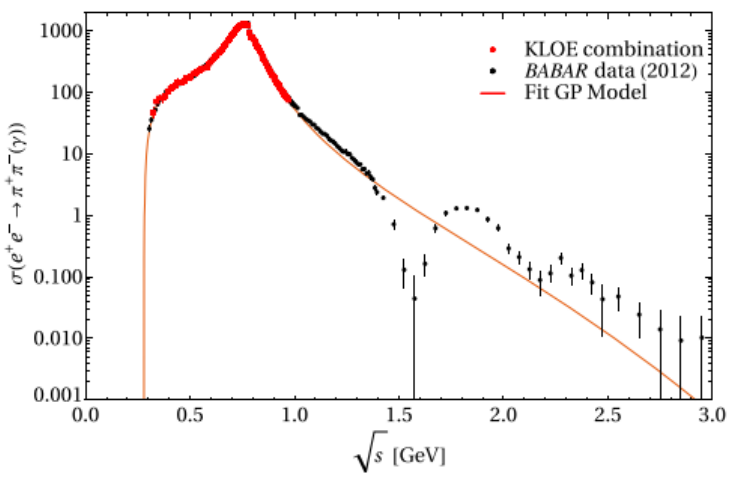
KLOE combination
BABAR data (2012)
Fit GP Model
$\sigma(e^+e^-\to\pi^+\pi^-(\gamma))$
$\sqrt{s}$ [GeV]

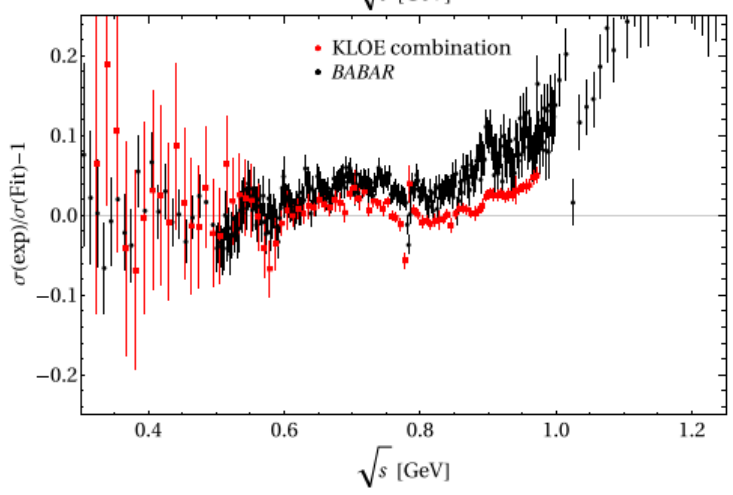
KLOE combination
BABAR
$\sigma(\text{exp})/\sigma(\text{Fit})-1$
$\sqrt{s}$ [GeV]

Fit results for the Seed model

	BABAR12 + Belle	KLOE12 + Belle	KLOEc + Belle	CMD3 + Belle	Global fit 1	Global fit 2
Data points	$337 + 62$	$60 + 62$	$85 + 62$	$209 + 62$	$337 + 60 + 209 + 62$	$337 + 85 + 209 + 62$
$\chi^2_{ee} + \chi^2_{\tau}$	$426.7 + 129.7$	$145.3 + 287.6$	$134.1 + 405.3$	$139.0 + 83.5$	$1455.6 + 207.1$	$2277.1 + 237.4$
χ^2	556.4	432.9	539.4	222.5	1662.7	2514.5
χ^2/d.o.f.	1.4	3.8	3.9	0.9	2.5	3.7
m_ρ	774.6 ± 0.1 MeV	774.1 ± 0.2 MeV	773.7 ± 0.1 MeV	773.6 ± 0.1 MeV	773.8 ± 0.1 MeV	773.5 ± 0.1 MeV
$\lvert\delta_{\rho\omega}\rvert$	$(2.5 \pm 0.0) \times 10^{-3}$	$(2.4 \pm 0.1) \times 10^{-3}$	$(2.3 \pm 0.1) \times 10^{-3}$	$(2.5 \pm 0.0) \times 10^{-3}$	$(2.4 \pm 0.0) \times 10^{-3}$	$(2.4 \pm 0.0) \times 10^{-3}$
$\arg[\delta_{\rho\omega}]$	$(13.5 \pm 1.0)°$	$(10.7 \pm 2.5)°$	$(16.8 \pm 2.3)°$	$(11.3 \pm 0.4)°$	$(9.1 \pm 0.4)°$	$(6.5 \pm 0.4)°$
$\lvert\delta_{\rho\phi}\rvert$	$0^\dagger$	$0^\dagger$	$0^\dagger$	$(2.8 \pm 0.2) \times 10^{-4}$	$(2.0 \pm 0.2) \times 10^{-4}$	$(2.1 \pm 0.3) \times 10^{-4}$
$\arg[\delta_{\rho\phi}]$	...	...	...	$(63.1 \pm 5.4)°$	$(58.2 \pm 6.3)°$	$(40.9 \pm 6.7)°$
$m_{\rho'}$	1397.2 ± 8.3 MeV	1413.8 ± 11.7 MeV	1406.3 ± 12.1 MeV	1449.2 ± 11.5 MeV	1414.5 ± 3.3 MeV	1369.4 ± 7.8 MeV
$\Gamma_{\rho'}$	324 ± 15 MeV	386 ± 28 MeV	447 ± 33 MeV	385 ± 28 MeV	231 ± 7 MeV	343 ± 16 MeV
$\mathrm{Re}[c_{\rho'}]$	$(9.2 \pm 0.5) \times 10^{-2}$	0.11 ± 0.01	0.12 ± 0.00	0.13 ± 0.01	$(3.1 \pm 0.5) \times 10^{-2}$	$(7.9 \pm 0.5) \times 10^{-2}$
$\mathrm{Im}[c_{\rho'}]$	$(-5.1 \pm 0.6) \times 10^{-2}$	$(-8.8 \pm 0.9) \times 10^{-2}$	-0.12 ± 0.01	$(-4.7 \pm 0.8) \times 10^{-2}$	0.19 ± 0.01	$(-7.2 \pm 0.5) \times 10^{-2}$
$m_{\rho''}$	1721.7 ± 10.5 MeV	$1730^\dagger$ MeV	$1730^\dagger$ MeV	$1730^\dagger$ MeV	1793.4 ± 6.7 MeV	1698.2 ± 10.6 MeV
$\Gamma_{\rho''}$	211 ± 12 MeV	$260^\dagger$ MeV	$260^\dagger$ MeV	$260^\dagger$ MeV	120 ± 6 MeV	203 ± 10 MeV
$\mathrm{Re}[c_{\rho''}]$	$(-8.1 \pm 0.5) \times 10^{-2}$	-0.11 ± 0.01	-0.12 ± 0.00	-0.11 ± 0.01	$(-2.7 \pm 0.4) \times 10^{-2}$	$(-7.3 \pm 0.5) \times 10^{-2}$
$\mathrm{Im}[c_{\rho''}]$	$(2.6 \pm 0.8) \times 10^{-2}$	$(4.1 \pm 0.8) \times 10^{-2}$	$(9.8 \pm 0.7) \times 10^{-2}$	$(2.0 \pm 0.7) \times 10^{-2}$	$(4.0 \pm 0.3) \times 10^{-2}$	$(4.5 \pm 0.8) \times 10^{-2}$

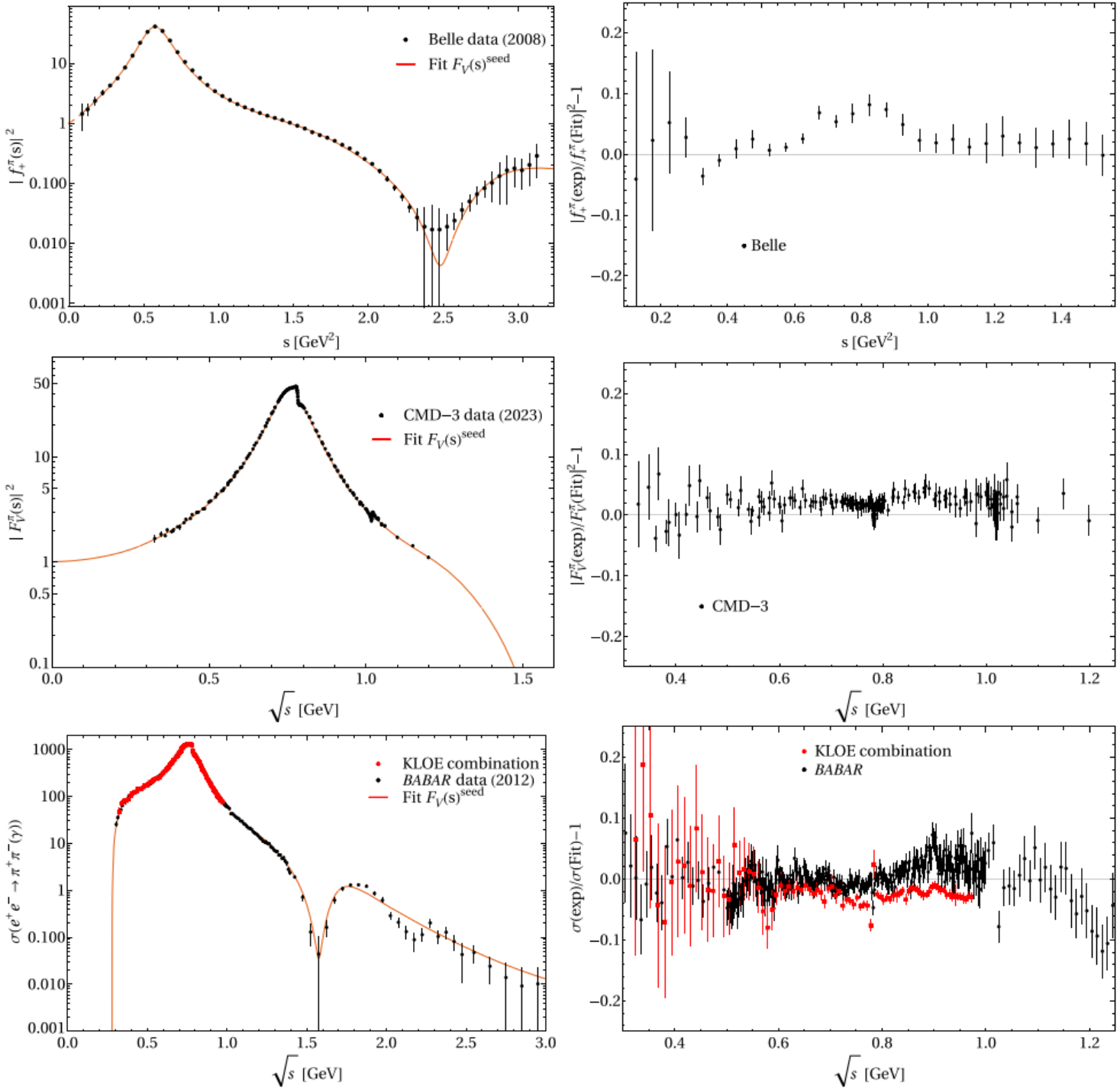
Belle data (2008)
Fit $F_V(s)^{seed}$
$|f_+^\pi(s)|^2$
s [GeV^2]
$|f_+^\pi(exp)/f_+^\pi(Fit)|^2-1$
Belle
CMD−3 data (2023)
$|F_V^\pi(s)|^2$
$\sqrt{s}$ [GeV]
$|F_V^\pi(exp)/F_V^\pi(Fit)|^2-1$
CMD−3
KLOE combination
BABAR data (2012)
$\sigma(e^+e^-\to\pi^+\pi^-(\gamma))$
BABAR
$\sigma(exp)/\sigma(Fit)-1$

CVC prediction of $B_{\pi\pi 0}$

- An important independent **cross-check** is provided by the **tau branching fraction**, another key quantity which can be directly **measured**.

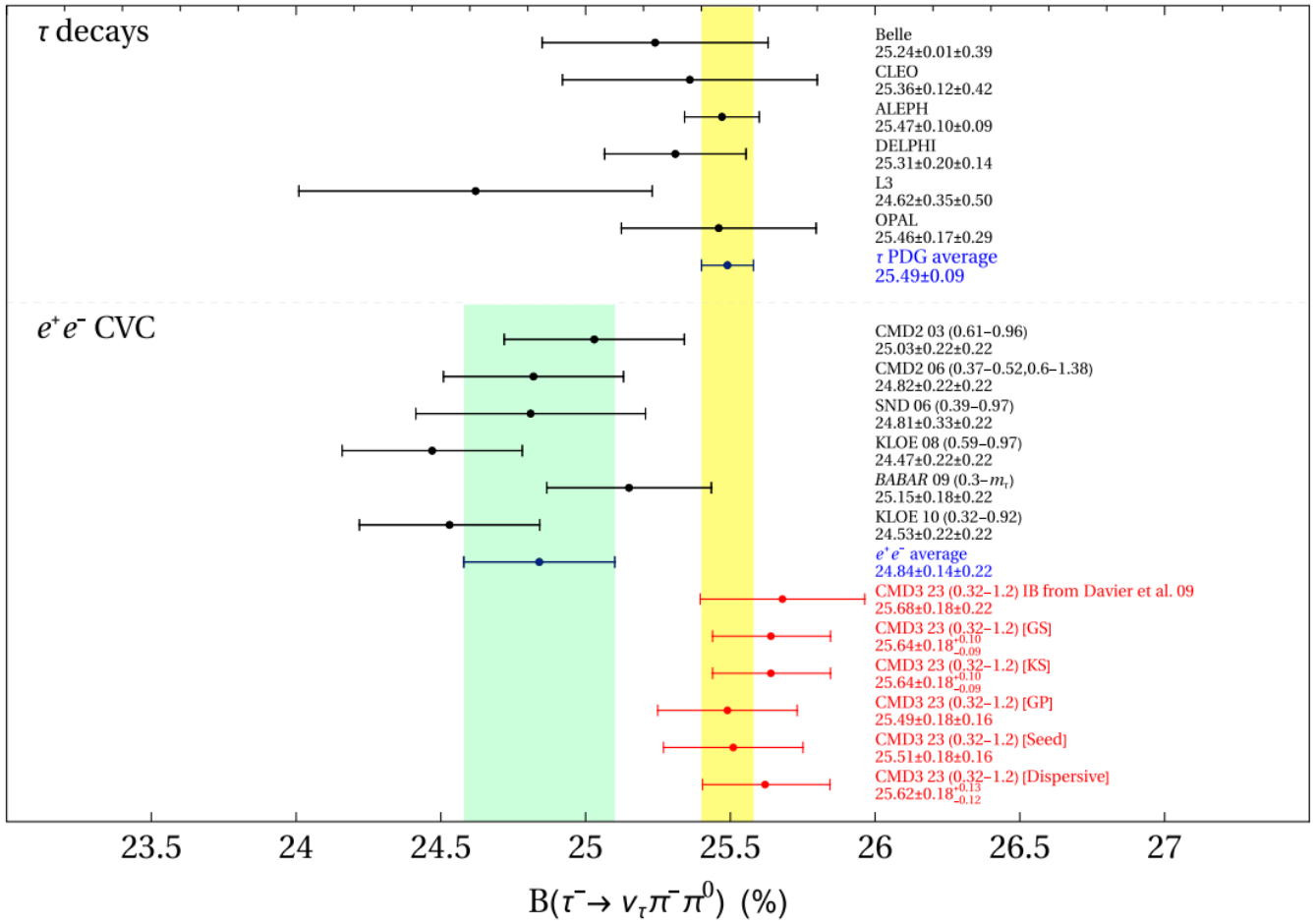

$$B_{\pi\pi^0}^{\mathrm{CVC}} = B_e \int_{4m_\pi^2}^{m_\tau^2} ds \sigma_{\pi^+\pi^-(\gamma)}(s) \mathcal{N}(s) \frac{S_{\mathrm{EW}}}{R_{\mathrm{IB}}(s)}$$

$$\mathcal{N}(s) = \frac{3|V_{ud}|^2}{2\pi\alpha_0^2 m_\tau^2} s \left(1 - \frac{s}{m_\tau^2}\right)^2 \left(1 + \frac{2s}{m_\tau^2}\right)$$

CMD-3. Phys.Rev.D 109 (2024) 11, 112002
Phys.Rev.D 111 (2025) 7, 073004

CVC prediction of $B_{\pi\pi 0}$

- An important independent **cross-check** is provided by the **tau branching fraction**, another key quantity which can be directly **measured**.

	$\Delta\mathcal{B}_{\pi\pi}^{\mathrm{CVC}}(10^{-2})$				
	GS	KS	GP	Seed	Dispersive
Source					p_{4-1}
S_{EW}			$+0.57(1)$		
G_{EM}			$-0.09\binom{3}{1}$		
FSR			$-0.19(2)$		
$m_{\pi^\pm} - m_{\pi^0}$ effect on σ			$+0.20$		
$m_{\pi^\pm} - m_{\pi^0}$ effect on Γ_ρ	-0.20	-0.22	-0.22	-0.24	-0.20
$m_{K^\pm} - m_{K^0}$ effect on Γ_ρ	$\cdots$	$\cdots$	-0.02	-0.02	$+0.01$
$m_{\rho^\pm} - m_{\rho^0}$ on Γ_ρ	$\cdots$	$\cdots$	$-0.12(11)$	$-0.12(11)$	$-0.10(9)$
$m_{\rho^\pm} - m_{\rho^0}$	$+0.09(8)$	$+0.09(8)$	$+0.12(11)$	$+0.12(11)$	$+0.08\binom{8}{7}$
$\rho - \omega$ interference	$-0.08(0)$	$-0.09(0)$	$-0.09(0)$	$-0.05(0)$	$-0.01(0)$
$\rho - \phi$ interference	$-0.00(0)$	$-0.00(0)$	$\cdots$	$-0.01(0)$	$-0.01(0)$
$\pi\pi\gamma$, electromagnetic decays	$+0.35(4)$	$+0.38(4)$	$+0.34(4)$	$+0.35(4)$	$+0.37(4)$
Total	$+0.65\binom{10}{9}$	$+0.65\binom{10}{9}$	$+0.50(16)$	$+0.52(16)$	$+0.63\binom{13}{12}\binom{3}{0}$

Phys.Rev.D 111 (2025) 7, 073004

Short-distance constraints

- For the parameters contributing to the leading-order chiral LECs:

$$F_V G_V = F^2, \qquad F_V^2 - F_A^2 = F^2,$$
$$F_V^2 M_V^2 = F_A^2 M_A^2, \qquad 4 c_d c_m = F^2,$$
$$8\left(c_m^2 - d_m^2\right) = F^2, \qquad c_m = c_d = \sqrt{2} d_m = F/2.$$

- For the even-intrinsic parity sector:

$$\lambda_{13}^P = 0, \quad \lambda_{17}^S = \lambda_{18}^S = 0,$$
$$\lambda_{17}^A = 0, \quad \lambda_{21}^V = \lambda_{22}^V = 0.$$

- The analysis of the <VAS> Green function yields:

$$\kappa_2^S = \kappa_{14}^A = 0, \quad \kappa_4^V = 2\kappa_{15}^V, \quad \kappa_6^{VA} = \frac{F^2}{32 F_A F_V},$$
$$F_V\left(2\kappa_1^{SV} + \kappa_2^{SV}\right) = 2 F_A \kappa_1^{SA} = \frac{F^2}{16\sqrt{2} c_m}.$$

Short-distance constraints

- The study of the <VAP> and <SPP> Green functions yield the following restrictions on the resonance couplings:

$$\sqrt{2}\lambda_0 = -4\lambda_1^{VA} - \lambda_2^{VA} - \frac{\lambda_4^{VA}}{2} - \lambda_5^{VA} = \frac{1}{2\sqrt{2}}\left(\lambda' + \lambda''\right),$$

$$\sqrt{2}\lambda' = \lambda_2^{VA} - \lambda_3^{VA} + \frac{\lambda_4^{VA}}{2} + \lambda_5^{VA} = \frac{M_A}{2M_V},$$

$$\sqrt{2}\lambda'' = \lambda_2^{VA} - \frac{\lambda_4^{VA}}{2} - \lambda_5^{VA} = \frac{M_A^2 - 2M_V^2}{2M_V M_A},$$

$$\lambda_1^{PV} = -4\lambda_2^{PV} = -\frac{F\sqrt{M_A^2 - M_V^2}}{4\sqrt{2}d_m M_A}, \quad \lambda_1^{PA} = \frac{F\sqrt{M_A^2 - M_V^2}}{16\sqrt{2}d_m M_V}.$$

- For the odd-intrinsic parity sector:

$$\kappa_{14}^V = \frac{N_C}{256\sqrt{2}\pi^2 F_V}, \quad 2\kappa_{12}^V + \kappa_{16}^V = -\frac{N_C}{32\sqrt{2}\pi^2 F_V}, \quad \kappa_{17}^V = -\frac{N_C}{64\sqrt{2}\pi^2 F_V}, \quad \kappa_5^P = 0,$$

$$\kappa_2^{VV} = \frac{F^2 + 16\sqrt{2}d_m F_V \kappa_3^{PV}}{32F_V^2} - \frac{N_C M_V^2}{512\pi^2 F_V^2}, \quad 8\kappa_2^{VV} - \kappa_3^{VV} = \frac{F^2}{8F_V^2}.$$

Fit results

- We perform a global fit using the relations for the resonance saturation of the anomalous sector LECs:

$$\kappa_1^V = (-2.1 \pm 0.7) \cdot 10^{-2}\ \text{GeV}^{-1},$$
$$\kappa_2^V = (-8.8 \pm 9.1) \cdot 10^{-3}\ \text{GeV}^{-1},$$
$$\kappa_3^V = (2.2 \pm 5.8) \cdot 10^{-3}\ \text{GeV}^{-1},$$
$$\kappa_6^V = (-2.1 \pm 0.3) \cdot 10^{-2}\ \text{GeV}^{-1},$$
$$\kappa_7^V = (1.2 \pm 0.5) \cdot 10^{-2}\ \text{GeV}^{-1},$$
$$\kappa_8^V = (3.1 \pm 0.9) \cdot 10^{-2}\ \text{GeV}^{-1},$$
$$\kappa_9^V = (-0.1 \pm 5.9) \cdot 10^{-3}\ \text{GeV}^{-1},$$
$$\kappa_{10}^V = (-5.9 \pm 9.6) \cdot 10^{-3}\ \text{GeV}^{-1},$$
$$\kappa_{11}^V = (-3.0 \pm 0.6) \cdot 10^{-2}\ \text{GeV}^{-1},$$
$$\kappa_{12}^V = (1.0 \pm 0.8) \cdot 10^{-2}\ \text{GeV}^{-1},$$
$$\kappa_{13}^V = (-5.3 \pm 1.1) \cdot 10^{-3}\ \text{GeV}^{-1},$$
$$\kappa_{18}^V = (4.7 \pm 0.8) \cdot 10^{-3}\ \text{GeV}^{-1}.$$

Phys.Rev.D 92 (2015) 025014
Phys. Rev. D 102 (2020) 114017

- These values are in good agreement with our earlier estimation $|\kappa^V_i| < 0.025\ \text{GeV}^{-1}$.

Summary of the current SM prediction for a_μ in comparison to experiment

WP24 - Phys. Rept. 1143 (2025) 1-158